



The impact of phase change material on photovoltaic thermal (PVT) systems: A numerical study

Sameh Alsaqoor^{a,b}, Ahmad Alqatamin^c, Ali Alahmer^{b,d,*}, Zhang Nan^c, Yaseen Al-Husban^e, Hussam Jouhara^{f,g}

^a Renewable Energy Technology Department, Faculty of Engineering and Technology, Applied Science Private University, Amman 11937, Jordan

^b Department of Mechanical Engineering, Faculty of Engineering, Tafila Technical University, P. O. Box 179, 66110, Tafila, Jordan

^c Department of Mechanical Engineering, Faculty of Engineering, Southwest Jiaotong University, Si Chuan Sheng, 610032, China

^d Department of Industrial and Systems Engineering, Auburn University, Auburn, AL 36849, United States

^e Renewable Energy Engineering Department, Faculty of Engineering, Isra University, P. O. Box 33, 11622 Amman, Jordan

^f Heat Pipe and Thermal Management Research Group, College of Engineering, Design and Physical Sciences, Brunel University London, UB8 3PH, United Kingdom

^g Vytautas Magnus University, Studentu Str. 11, LT-53362, Akademija, Kaunas Distr, Lithuania

ARTICLE INFO

Keywords:

Phase change material (PCM)

Photovoltaic thermal (PVT)

Thermal energy storage

Photovoltaic efficiency

PVT-PCM

ABSTRACT

This study examines the impact of incorporating phase change material (PCM) in photovoltaic thermal (PVT) systems on their electrical and thermal performance. Although PVT systems have shown effectiveness in converting solar energy into both electricity and heat, there is a necessity for studies to investigate how integrating PCMs can further enhance performance. The study also aims to explore the effect of solar irradiation and coolant mass flow rate on the electrical and thermal output of both PVT and PVT-PCM systems. A graphical user interface was developed within the MATLAB Simulink under the weather conditions of Amman, Jordan. The results show that the incorporation of PCM in PVT systems significantly reduces solar cell temperature and increases electrical efficiency. The highest electrical efficiency of a PVT system with PCM was found to be 14%, compared to 13.75% in a PVT system without PCM. Furthermore, the maximum achievable electrical power in a PVT system with PCM was 21 kW, while in the PVT system without PCM it was 18 kW. The study also found that increasing the coolant mass flow rate in a PVT system with PCM further reduced PV cell temperature and increased electrical efficiency, while the electrical efficiency of both the PVT and PVT-PCM systems decreases as solar incident radiation flux increases, resulting in a significant rise in cell temperature. At an increased solar radiation level from 500 W/m² to 1000 W/m², the electrical efficiency of the PVT configuration decreases from 13.75% to 11.1%, while the electrical efficiency of the PVT-PCM configuration falls from 14% to 12%. The findings of this study indicate that the use of PCM in PVT systems can lead to significant improvements in energy production and cooling processes. The results provide valuable information for designing and optimizing PVT-PCM systems.

1. Introduction

Photovoltaic (PV) cells are inefficient in converting solar energy into electricity. Commercial solar panels have yet to achieve a maximum efficiency of more than 20% [1]. As a result, 80% of the energy obtained is lost as heat [2]. One of the most challenging aspects of this characteristic is the increase in the Tsc, which affects the power produced and, as a result, the efficiency of the solar cell [3]. As a result, to enhance PV cell efficiency, the temperature of the cells must be kept low, around typical test conditions (25 °C) [4]. The simplest and best way to handle this problem is to utilize a hybrid PV system with a thermal collector,

which absorbs thermal energy (E_{th}) and so lowers the Tsc [5,6]. This combination led to an increase in power generation, as well as an increase in the η_e [7]. Phase change materials (PCMs) have numerous applications, including PVT systems. In PVT systems, PCMs are utilized to regulate and store thermal energy to achieve the highest possible electrical η_e and E_{th} [8]. PCMs have a broad range of applications beyond PVT systems, such as thermal energy storage [9], battery thermal management [10], electronics cooling [11], automobiles [12], and cold chain management [13]. When used in PVT configurations, PCMs offer the additional benefit of storing heat and reducing PV cell temperatures compared to PVT systems without PCMs. In comparison to PVT configurations without PCMs, the PCM used in PVT provides an

* Corresponding author.

E-mail address: aza0300@auburn.edu (A. Alahmer).

Nomenclature			
A	Area (m^2)	ρ	Density ($kg.m^{-3}$)
C, C_p	Specific heat ($J kg^{-1} K^{-1}$)	σ	Stefan- Boltzmann constant
E	Energy (W)	τ	Transmittance coefficient
G	Solar irradiation (Wm^{-2})		
h	Convective heat transfer coefficient ($Wm^{-2} K^{-1}$)	<i>Subscript</i>	
Nu	Nusselt number	o	Overall
mf	mass flow rate (kg/sec)	amb	Ambient
PCM	Phase change material	cond	Conduction
PV	Photovoltaic	conv	Convective
PVT	Photovoltaic thermal	e	Electrical
R_e	Reynolds number	env	Environment
T	Temperature ($^{\circ}C$)	g	Glass
U	Overall heat transfer coefficient ($Wm^{-2} K^{-1}$)	ins	Insulation
f	contact factor	pv	Photovoltaic
k	Thermal conductivity ($Wm^{-1}K^{-1}$)	r	Reference
p	Packing factor	sc	Solar cell
α	Absorption	td	Tedlar
δ	Thickness (m)	th	Thermal
η	Efficiency	w	Wind
μ	Viscosity ($N.s.m^{-2}$)	abs	Absorber
		f	Fluid

extra benefit in storing heat and lowering PV cell temperatures. The latent heat of the PCMs is rather high. When the material's transition temperature from solid to liquid is reached, this enables the material to store latent heat. However, as it transitions from liquid to solid form, it releases latent heat into the environment in a cooler setting. PCM, in any situation, retains sensible heat in the same way that a continuous solid or liquid phase does [14,15]. Furthermore, the integrated PCM in PVT has additional benefits, including a large heat capacity, no energy required for circulation, non-corrosive and nontoxic properties, and the thermal energy stored may be utilized at night [16].

Hasan et al. [17] examined the temperature response of solar panel PVs to a PV-PCM configuration. Five PCMs were tested, with melting temperatures around 25 ± 4 $^{\circ}C$ and a latent heat of fusion of between 140 and 213 kJ/kg. The PV-PCM system maintained a temperature substantially lower than the PV reference T_{sc} on a clear day with considerable and active sunlight for about 10 h. The results showed a maximum temperature reduction of 18 $^{\circ}C$ for 30 min and a sustained 10 $^{\circ}C$ temperature reduction for 5 h at 1000 W/m^2 insolation. Tan [18] utilized TRNSYS software to study the influence of PCM on a concentrated solar collector both experimentally and numerically. According to the research findings, the PV with PCM has a 35.6 $^{\circ}C$ lower temperature than the PV without PCM. Furthermore, employing PCM resulted in a 7.3% increase in electricity efficiency over a one-year cycle. Preet et al. [19] conducted an experimental study to enhance the performance of PV systems. They examined three systems: a traditional PV panel, a water-based PV/thermal system with a double absorber plate, and a water-based PV/thermal system with PCM. The findings suggested that using PV/thermal technology may improve the efficiency of both electrical and thermal systems. The study also analyzed the effect of various mass flow rates on the efficiency of these systems. Alzaabi et al. [20] proposed adopting a water hybrid PVT configuration to boost η_e and thermal efficiency (η_{th}) of PV systems under UAE climatic conditions. The study showed that adopting the circulating water through the collector at the backside of the PV panel significantly reduced the temperature by 10–20 $^{\circ}C$ during the afternoon, resulting in a 15% to 20% increase in the electrical output power. Furthermore, during system operation, the thermal efficiency can attain 60% to 70%. Naseer et al. [21] investigated the impact of varying the thickness of hybrid PCMs on the performance of PV panels in Taxila, Pakistan. The PV module was sandwiched between two PCMs with different melting points separated

by an aluminum plate. Three configurations were compared to the natural cooling configuration. The configuration with the lower melting point PCM showed better performance. The highest thickness of low melting PCM resulted in an average temperature reduction of 8.1 $^{\circ}C$ and an increase in electrical efficiency of 7.8%.

Nardi et al. [22] evaluated the effect of environmental factors on the overall efficiency (η_o) of the PVT system. The η_e and η_{th} of a commercial PVT module, as well as infrared thermographic diagnostics, were studied using both non-cooling and cooling scenarios. The experiments were carried out throughout the summer with the goal of determining the impact of the environment on system efficiency. Seven experiments were carried out under various situations. According to the findings of the experiments, the configuration with a flat reflector in front of the module and no cooling had the highest temperatures, followed by the setup with no cooling and no reflector. Moreover, the authors claim that the η_{th} and η_o increased significantly as a result of the setup's simplicity. They concluded that utilizing a basic reflector can result in a significant increase of 28% in electrical efficiency. Liang et al. [23] carried out experiments to assess the performance of a conventional PV and a graphite-filled PVT solar collector. In terms of η_e and primary energy-saving efficiency, the results reveal that the graphite-filled PVT solar system surpasses conventional PV systems. The highest electrical efficiency and primary energy-saving efficiency of the PVT collector filled with graphite were 7.2% and 48%, respectively. The outputs of four distinct types of PVT collectors in terms of sheet-tube, channel, free flow, and two absorbers of PVT collector were examined by Zondag et al. [24]. The η_{th} and η_e were examined in addition to the yearly production of hot water. Although the sheet-tube of PVT collectors was not the most effective device when compared to the others, it was the best choice due to its ease of fabrication. Furthermore, the results indicated that the uncovered collector has a η_{th} of 52% at zero reduced temperature. However, the single cover sheet-and-tube design has a η_{th} of 58%, while the channel above PV design exhibits the highest η_{th} at 65%. According to Wu et al. [25], modeling a PVT device with water as the transfer fluid might result in η_{th} and η_e exceeding 63.65% and 8.45%, respectively. Using air as the coolant in a conduit at the rear of the panel to cool a PVT arrangement yielded 7.3% more energy than without cooling the system.

The PVT systems have been combined with PCM to innovate a new system known as PVT-PCM. Due to material preferences where the

substance can release and absorb appropriate energy to offer beneficial heating and cooling, the new system is projected to boost energy production and cooling processes significantly. Within the PVT there are several types of cooling systems, including water cooling and air cooling (both are utilized), as well as water heating in the winter.

Hassan et al. [26] explored using a PCM to control the PV system temperatures. In the United Arab Emirates, where there are hot conditions for most of the year, the authors installed five PV systems. Four of these systems used various PV-PCM cells, which were all tested for their impact on system functioning to ensure that they were acceptable for use in a PV-PCM system. According to the study, the highest reduction in peak temperature achieved by utilizing PCM was 5 °C on a foggy day and 11 °C on a clear sky day. Yang et al. [27] constructed a hybrid PVT-PCM platform to evaluate η_{th} and η_e , compared with a traditional (PVT) configuration. The study found that integrating PCM and PVT improves the envisioned system's overall η_{th} and η_e . Furthermore, it was observed that incorporating a PCM layer into a PVT panel significantly reduces the amount of heat lost to ambient. When the radiation is less intense or insufficient, the heat absorbed in the PCM can be liberated into the working fluid, increasing its lifespan to the desired building.

Through the utilization of the PCM layer for cooling, the PVT-PCM module enhances its electrical efficiency, with the PVT-PCM system achieving a higher solar η_e of 8.16% compared to 6.98% for the PVT system. Browne et al. [28] tested a PVT-PCM system's performance in a controlled indoor setting. Compared to a PVT system, the time needed to store heat was nearly twice as long under the same conditions. Likewise, the water temperature increase in the PVT-PCM system was around 6 °C higher than in the PV/T system. The performance of a PVT-PCM system increases significantly. The potential for heat storage increases by 100% in regions with higher temperatures. Ahmadi et al. [29] studied the impact of passive and active cooling methods on the electrical and thermal performance of PVT system under varying solar radiation levels. They utilized PCM in the passive cooling system by infusing it into a heat conductive foam. Results revealed that the PCM-composite system could improve electrical efficiency by up to 14% and reduce PV-cell temperature by up to 6.8% (approximately 4 °C). Additionally, active cooling was evaluated by circulating water through a cooling block under the PVT system. The PV-PCM-composite system with active cooling achieved the highest energy efficiencies ranging from 66.8 to 82.6%. Dogkas et al. [30] investigated the use of organic PCMs in a cold heat storage system. It was found that the process of melting and solidification could be shortened and that a higher heat transfer rate could be attained. Righetti et al. [31] investigated how to improve the effective thermal conductivity of RT70 paraffin wax, which has a phase transition temperature of 70 °C. In practice, the optimal shape has been determined, and a relationship between charging time and thermal boost has been suggested.

A one-dimensional thermal energy balance framework for PVT-PCM was simulated by Malvi et al. [32]. According to the research outcomes, PCM boosts PV production by 9% and raises the temperature of the water on average by 20 °C. Bhakre et al. [33] developed a 2-D computational model to investigate the performance of a PVT-PCM system with different water container thicknesses (WCT) and system orientations. The optimal WCT was found to be 30 mm, and increasing the system orientation from 30° to 90° resulted in a decrease in the average temperature of the PV panel and PCM, leading to an increase in average electrical efficiency of 14.93% and 1.35% at 30° and 90° system orientations, respectively. Hamid et al. [34] conducted a 3D numerical simulation to compare the performance of PVT structures with and without PCM, using water as a coolant. The study included six different configurations, with buried water pipes and an additional PCM layer with different melting temperatures. Results indicated that burying water pipes inside the PCM improved overall performance. The glazed and unglazed PV/T modules integrated with dual PCMs achieved the highest daily average energetic and exergetic efficiencies.

In the meteorological situations of Lyon, France, Gaur et al. [35]

examined the PVT technique with and without PCM computationally. A thermal model was developed to investigate the temperatures of different input components. Under winter environmental conditions, the η_e of photovoltaic panels of PVT collectors with or free of PCM were measured to be 16.87% and 16.5%, respectively. This analysis was conducted at a particular ambient temperature (T_{amb}) and solar irradiation. The performance of a solar PVT-PCM system under Malaysian weather conditions was developed and analyzed by Hossain et al. [36]. The study revealed that using PCMs enhanced both electrical and thermal efficiency, with maximum efficiencies of 14.57% and 15.32% for PVT and 75.29% and 86.19% for PVT-PCM, respectively. A novel design for a PVT collector was tested in a Mediterranean climate by Jurčević et al. [37]. The design was evaluated for performance, economic and environmental aspects. The PVT collector consisted of four cooling blocks with water as the working fluid and organic PCM in plexiglass containers. The system achieved an overall energy efficiency of 62.2%, with an estimated annual efficiency of less than 50%. The leveled cost of energy was between 0.056 to 0.083 €/kWh. Hosseinzadeh et al. [38] studied the PVT in conjunction with PCM and a ZnO/water nanofluid working fluid to compute η_{th} and η_e experimentally. Using PCM, the production thermal intensity of the PVT with nanofluid was raised by 29.6% in August and September under the climatic circumstances of Mashhad, Iran. In addition, the proposed system had the highest average exergy performance of 13.61%. Riehl and Mancin [39] examined the effect of a specific solid nanoparticle in the base fluid, and the results were obtained in order to develop models that predicted nano-liquid characteristics. Unfortunately, these models still provide inconsistent findings for identical parameters of solid nanoparticles and base fluid, resulting in inaccurate data. Al-Musawi et al. [40] investigated the effects of pure water, SiO₂/water nanofluid, and a PCM on the performance of PVT. The study compared two PVT modules, one with PCM and one without. The results showed that using a water-based PVT/PCM reduced the average PV cell temperature by 16 °C, leading to an 8% increase in electrical efficiency and a 25% increase in thermal efficiency. The study suggested that increasing the melting temperature of the PCM enhanced the thermal efficiency of the PVT/PCM system. Asefi et al. [41] investigated the utilization of porous materials to enhance the effectiveness of PVT-PCM systems. The study revealed that porous materials could enhance the thermophysical properties of PCMs and enhance the distribution of PV temperature, leading to improved electrical and thermal efficiency. A 3D numerical model was employed to analyze the system's efficiency with different working fluids and porous materials. The findings suggested that replacing pure PCM and water with nanofluids and porous PCM significantly boosts the efficiency of PVT-PCM. Khodadadi and Sheikholeslami [42] analyzed the efficiency of a PVT-PCM system with multiple finned containers. The results showed that increasing the number of fins improved heat transfer into the PCM, increased the melting rate, and lowered the average surface temperature. The inclusion of nano-powders in paraffin increased the liquefied fraction by 2.13% when compared to pure PCM.

Although there have been studies on the impact of PCM on PVT systems, there is still a need to investigate the effect of PCM on the thermal energy storage and thermal efficiency of PVT-PCM systems. While PVT systems have been shown to be effective in converting solar energy into both electricity and heat, there is a lack of research on how the integration of PCMs can further improve the performance of these systems. Additionally, there is a need to investigate the impact of coolant mass flow rate on the electrical and thermal performance of PVT and PVT-PCM systems. The main objective of this study is to develop and analyze the performance of a new integrated system called PVT-PCM, which combines photovoltaic thermal (PVT) systems with phase change materials (PCMs). Furthermore, it investigates the impact of PCMs on PVT systems by performing a comprehensive comparison between a PVT system without PCM and an integrated PVT-PCM system. The study aims to compare the thermal and electrical efficiencies of the PVT-PCM system with those of a conventional PVT system without PCM

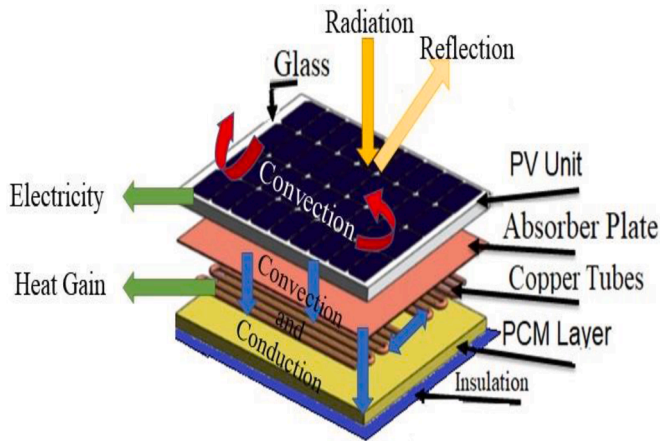


Fig. 1. Configuration of the PVT-PCM module showing heat transfer modes.

under the weather conditions of Amman, Jordan. Additionally, the study aims to investigate the impact of PCM on the thermal energy storage and thermal efficiency of PVT-PCM systems, as well as the effect of coolant mass flow rate on the electrical and thermal output of PVT and PVT-PCM systems, which can provide valuable information for designing and optimizing PVT-PCM systems. The ultimate goal is to provide new insights into the potential benefits of integrating PCMs in PVT systems and to identify ways to further improve their performance. The study uses a graphical user interface developed within the MATLAB Simulink program and investigates the thermal and electrical efficiencies of the PVT-PCM system under the weather conditions of Amman, Jordan. To the best of our knowledge, this is the first study that investigates the use of PCM in a PVT system under the weather condition of Amman, Jordan, which is characterized by high solar radiation and high temperature. The results of this study will provide valuable insights for future research and the design of PVT-PCM systems.

2. Methodology

The electrical and thermal efficiencies of both PVT and PVT-PCM hybrid configurations were simulated and compared using the MATLAB program. The two systems were studied numerically with irradiances varying between 500 and 1000 W/m², mass flow rate (mf) ranging from 0.7 to 0.95 kg/s at a temperature of 25 °C. The use of PCM in PVT systems offers great advantages in the form of PV cell cooling and heat conservation. In the first system, a thermal collector was connected to a PV without a PCM in order to build a PVT system, whereas, in the second system, a PCM was used to construct the PVT-PCM for numerical assessment.

The following assumptions underpin the mathematical model that was used to simulate the PVT system [43–46]:

- The temperature of the working fluid in the collector fluctuates axially, that is, solely in one direction.
- Compared to the electrical output, the ohmic losses of the solar cells are negligible.
- The sky is considered to be a black body with a given temperature.
- The thermal-physical parameters of the absorber plate, collector tub, and PV layers remain constant and independent of temperature.
- PVT/PCM systems have negligible contact resistance among solid components.
- In the numerical simulation, parameters of the PCM, such as melting temperature and thermal conductivity, are considered constant.
- No dust on the surface of the PV will impact solar energy absorption.
- PCM is homogenous and isotropic in both liquid and solid phases.

2.1. System description

This system is constructed from a PVT collector integrated with PCM material, a heat exchanger for the storage tank, a standby boiler, two pumps, a flow meter, and numerous sensors at different locations, including thermocouples, pyranometer, multimeter, and flow meter to measure temperatures, solar irradiation, voltage and current, and fluid flow rate respectively. A transparent glass cover with high transmittance of more than 95%, a PV unit, a group of round copper tubes combined with a layer of PCM, and an insulating layer beneath the solar panel to prevent heat leakage are all included in this model. The PVT-PCM configuration is shown in Fig. 1.

The storage tank is built from a combination of galvanized steel and PCM. To avoid heat leaking into the environment, it is separated from the exterior using glass wool. Because of their low cost and superior thermal conductivity, copper and galvanized steel were used [47]. A heat exchanger is employed to transmit heat from the working fluid to the household water.

Throughout the day, solar radiation strikes the PV unit's surface; some of it converts to electricity, some is reflected, while the rest converts to E_{th} . The copper tubes gather heat and warm the fluid inside the PV unit, and the PCM stores a portion of this energy for use when solar radiation is insufficient or unavailable.

A heat exchanger is used in the PVT-PCM and PVT schemes to cool down the operating fluids in a closed loop. Following the absorption of heat from the PV panel, it transmits the heat to the domestic water, which is stored in a tank embedded with PCM. A supplementary boiler system was employed to provide E_{th} during the night or when there is no solar irradiance on the PV module's surfaces.

Two alternative systems were used in this study, both of which are polycrystalline silicon photovoltaics. The first is a solar system with a thermal collector made of copper tubing (PVT). The second system is similar to the first, except that PCM surrounds the collector (PVT-PCM). The η_e and η_{th} of both proposed systems were assessed. A schematic of the two systems is illustrated in Fig. 2. Table 1 presents the PV that was utilized in this investigation.

2.2. PCM thermophysical characteristic materials

Compounds with the ability to absorb and release a considerable amount of latent thermal energy by transitioning from one phase to another (solid/liquid) across a limited temperature range are known as phase change materials (PCM). These materials go through several stages in which their physical states change in the solid and liquid states [48,49]. The thermophysical characteristics of Lauric acid [50,51], employed in this work, are shown in Table 2. As displayed in Table 2, Lauric acid has a melting point of 43.8 °C and a boiling point of 297.9 °C. Therefore, it can be used as a PCM for thermal energy storage applications in the temperature range of 20–50 °C. Lauric acid has been shown to have good thermal stability and heat storage capacity. It is worth noting that the transition temperature is expected to affect the productivity of PV-PCM or PVT-PCM systems. The PV and water pipes will share the heat with the PCM. In a typical PV, the backboard temperature is between 30 and 80 °C. The PCM has been added to the PV to effectively bring down the PV's temperature while increasing its electrical output. To achieve an acceptable temperature differential between the PCM layer and the water pipe, it is important that the melting temperature of lauric acid is not too low. Therefore, we adopted lauric acid in this study since the melting temperature of lauric acid is 40–45 °C, with high latent heat, strong thermal and chemical stability, and almost no supercooling or contamination [52]. It has been often synthesized with other PCMs and used in engineering because its excellent phase change temperature makes it suitable for solar energy applications.

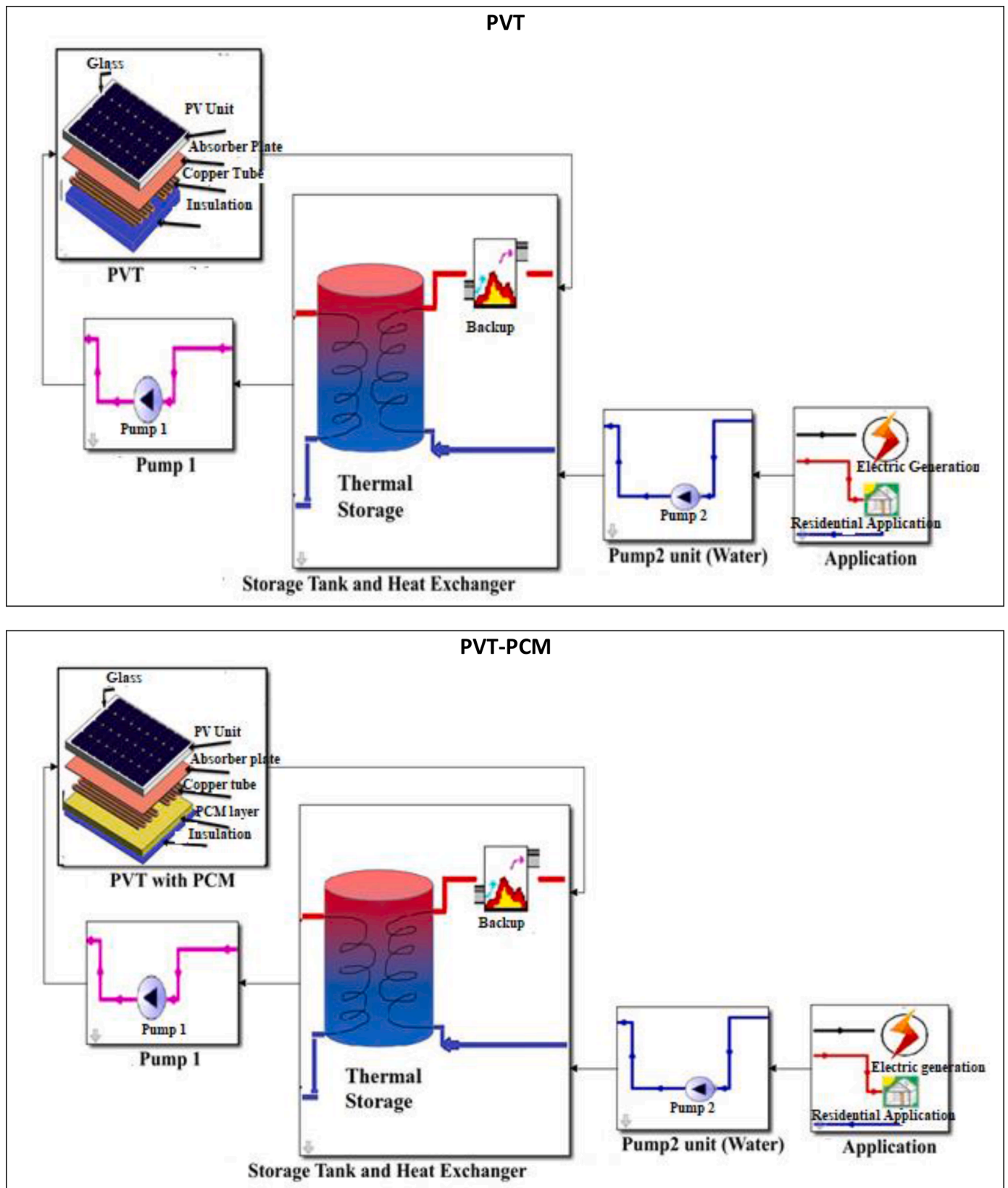


Fig. 2. Arrangement of the (a) PVT, and (b) PVT-PCM.

3. Mathematical modeling

The system output parameters in terms of η_e and η_{th} are quantified using data obtained through computational modeling, such as

temperatures of various portions of the systems, solar irradiations, and mass flow rates.

The entire amount of energy absorbed by the module's top surface (E_{tot}) can be calculated as follows from Eq. 1 [53]

Table 1
Properties of the PV module used.

Item	Specification
Materials	Polycrystalline silicon
Area of a cell	0.015 m ²
Number of modules	150
Short-circuit current	4 A
Open circuit voltage	70 V
STC	1000 W/m ² , AM 1.5, 25 °C
PCM layer thickness	10 mm
Tube diameter	12.5 mm
Tube number	25

Table 2
Thermophysical properties of Lauric acid.

Property	Liquid	Solid
Melting temperature (°C)	43.3	
Specific heat (kJ/kg.K)	2.20	1.95
Thermal conductivity (W/m.K)	0.15	0.45
Viscosity (kg/m.s)	0.0006	
Volumetric expansion (K ⁻¹)	9.10 ⁻⁴	
Melting latent heat (kJ/kg)	187.2	

$$E_{tot} = \tau_g \alpha_{sc} p_{sc} GA \quad (1)$$

where τ_g is Transmittance coefficient of the glass cover, α_{sc} is Absorptivity of solar cell, p_{sc} is Packing factor of solar cell, G is Solar irradiation (Wm⁻²), A is PV Area (m²).

The convection energy loss at the module's top surface (E_l) was evaluated as follows from Eq. 2

$$E_l = U_{sca} (T_{sc} - T_{amb}) A \quad (2)$$

where U_{sca} is Overall heat transfer coefficient from top surface of module to ambient through glass cover (Wm⁻² K⁻¹).

The electrical power (E_e) generated from the solar cell's absorbed energy was computed using Eq. 3 [54]:

$$E_e = \eta_{sc} p_{sc} \tau_g \alpha_{sc} GA [1 - \mu_{sc} (T_{sc} - T_r)] \quad (3)$$

where η_{sc} is solar module's electrical efficiency, μ_{sc} is Temperature coefficient of PV, T_r is Reference temperature.

Eq. 4 is used to calculate the energy transmitted to the module's bottom surface.

$$E_{th} = U_{td} (T_{sc} - T_{td}) A \quad (4)$$

where E_{th} is Energy from thermal collector (W), U_{td} is Heat transmission coefficient from glass to Tedlar (Wm⁻² K⁻¹), T_{td} is Temperature of the Tedlar (°C)

Total energy transfer from the top glass to Tedlar and the atmosphere can be evaluated by the use of the conservation of energy principle.

$$E_{tot} = E_l + E_{th} + E_e \quad (5)$$

The temperature of solar cells can be calculated using Eq. 6 [55]:

$$T_{sc} = \frac{p_{sc} G (\tau_g \alpha_{sc} - \eta_{sc}) + (U_{sca} T_a + U_t T_{td})}{(U_{sca} + U_t)} \quad (6)$$

The η_e , η_{th} , and η_o of a PV system, may be calculated using the formulas of Eq. 7, Eq. 8, and Eq. 9 respectively.

$$\eta_e = \frac{\text{Produced electrical power}}{\text{Total received energy}} = \frac{E_e}{E_{tot}} \quad (7)$$

$$\eta_{th} = \frac{\text{Extracted thermal energy}}{\text{Total received energy}} = \frac{E_{th}}{E_{tot}} \quad (8)$$

$$\eta_o = \frac{E_e + E_{th}}{E_{tot}} \quad (9)$$

The following are the detailed energy balance equations for the subsystems [46]:

For glass

$$\rho_g \delta_g C_g \frac{dT_g}{dt} = \alpha_g G + h_{rad.g \rightarrow env} (T_{sky} - T_g) + h_w (T_{amb} - T_g) + h_{cond.g \rightarrow pv} (T_{pv} - T_g) \quad (10)$$

where ρ_g is glass density (kg.m⁻³), δ_g is glass thickness (m), T_{sky} is temperature of the sky (°C), C_g is glass specific heat (J kg⁻¹ K⁻¹), α_g is Absorption of glass, $h_{rad.g \rightarrow env}$ is equivalent irradiation coefficient between the PV and the sky (Wm⁻² K⁻¹), h_w is convection coefficient due to the wind (Wm⁻² K⁻¹), $h_{cond.g \rightarrow pv}$ is equivalent conduction coefficient between glass and PV (Wm⁻² K⁻¹).

The transient energy variations in the cover glass are represented on the left side. The first term on the right-hand side of the equation is the irradiation collected by the glass cover; the next term is the radiation between the cover glass and ambient; the third term is the convection between the cover glass and the outside; and the fourth term is the conduction from the PV cells to the cover glass.

For photovoltaic panel

$$\rho_{pv} \delta_{pv} C_{pv} \frac{dT_{pv}}{dt} = \alpha_{pv} \tau_g G - E_{elec} + h_{cond.pv \rightarrow g} (T_g - T_{pv}) + h_{cond.pv \rightarrow abs} (T_{abs} - T_{pv}) \quad (11)$$

where ρ_{pv} is a PV density (kg.m⁻³), δ_{pv} is Thickness of PV (m), C_{pv} is PV specific heat (J kg⁻¹ K⁻¹), α_{pv} is Absorption of PV, $h_{cond.pv \rightarrow g}$ is equivalent conduction coefficient between the PV and the glass (Wm⁻² K⁻¹), $h_{cond.pv \rightarrow abs}$ is equivalent conduction coefficient between the PV and the absorber plate (Wm⁻² K⁻¹), T_{abs} is absorber plate temperature (°C), T_{pv} is PV temperature (°C).

For absorber plate

$$\rho_{abs} \delta_{abs} C_{abs} \frac{dT_{abs}}{dt} = h_{conv.pv \rightarrow abs} (T_{abs} - T_{pv}) + f_{abs,tube} h_{cond.abs \rightarrow tube} (T_{tube} - T_{abs}) + f_{abs,ins} h_{cond.abs \rightarrow ins} (T_{ins} - T_{abs}) \quad (12)$$

where ρ_{abs} is absorber plate density (kg.m⁻³), δ_{abs} is absorber thickness (m), C_{abs} is absorber specific heat (J kg⁻¹ K⁻¹), $h_{cond.pv \rightarrow abs}$ is equivalent conduction coefficient between PV and absorber (Wm⁻² K⁻¹), $h_{cond.abs \rightarrow tube}$ is equivalent conduction coefficient between absorber and tube (Wm⁻² K⁻¹), $f_{abs,tube}$ is the contact factor of the absorber and tube, which is equal to one in contact parts or zero in noncontact. Between the absorber and the insulation, a comparable factor may be defined as $f_{abs,ins}$, T_{abs} is absorber temperature (°C), T_{ins} is insulation temperature (°C).

For tubes

$$\rho_{tube} \delta_{tube} P dy C_{tube} \frac{dT_{tube}}{dt} = A_{abs,tube} h_{cond.abs \rightarrow tube} (T_{tube} - T_{abs}) + h_{conv,tube \rightarrow f} P dy (T_f - T_{tube}) + A_{ins,tube} h_{cond,tube \rightarrow ins} (T_{ins} - T_{tube}) \quad (13)$$

where ρ_{tube} is tube density (kg.m⁻³), δ_{tube} is tube thickness (m), C_{tube} is tube specific heat (J kg⁻¹ K⁻¹), $h_{cond,tube \rightarrow f}$ is equivalent conduction coefficient between the tubes and the fluid (Wm⁻² K⁻¹), $h_{cond,tube \rightarrow ins}$ is equivalent conduction coefficient between the tubes and the insulation (Wm⁻² K⁻¹), P is perimeter

For working fluid

$$\rho_f A_f dy C_f \frac{dT_f}{dt} = h_{conv,tube \rightarrow f} P dy (T_{tube} - T_f) \quad (14)$$

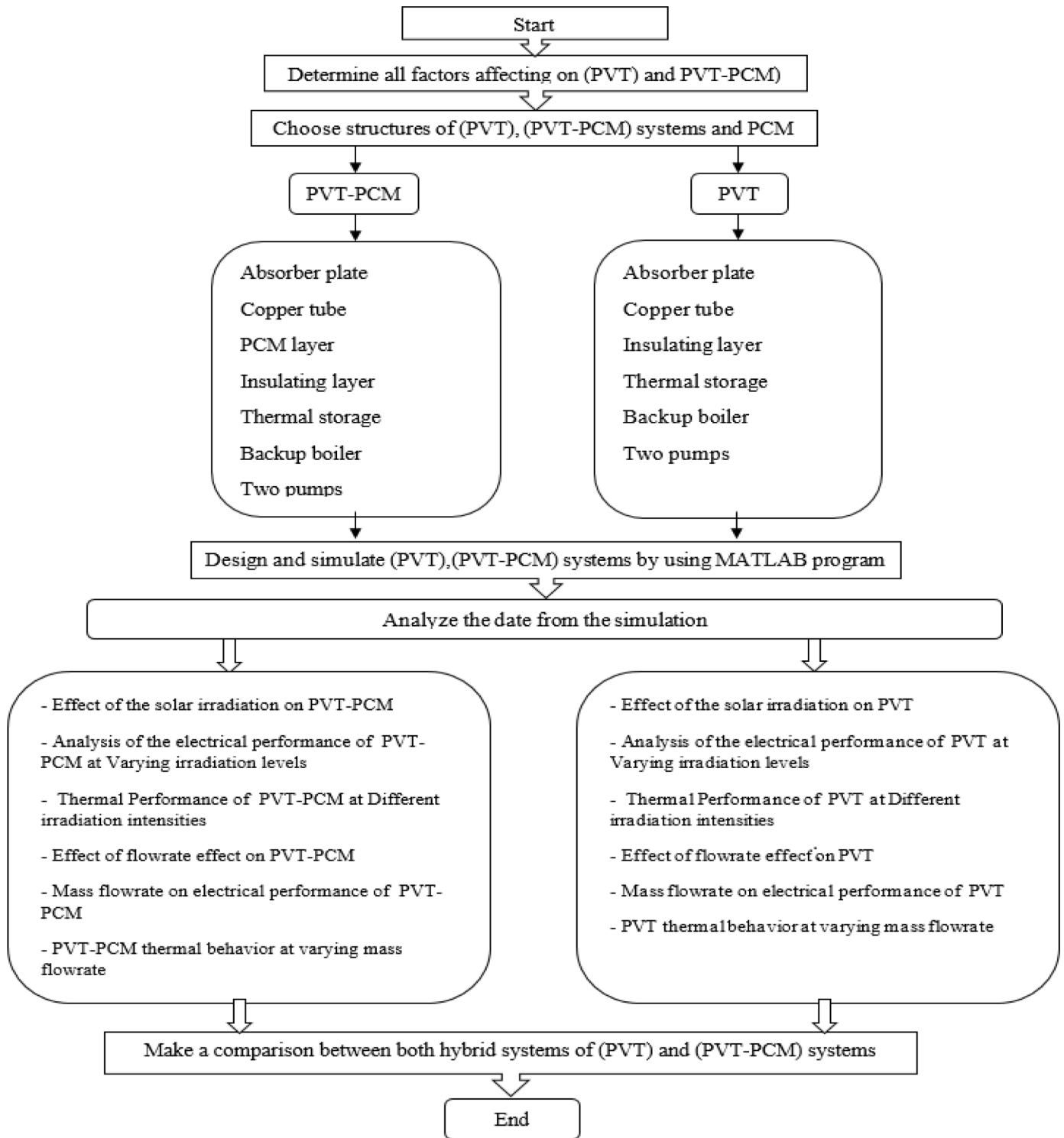


Fig. 3. The following procedures were executed to compare the electrical and thermal efficiencies of PVT systems with and without PCM under various solar irradiation levels and mass flowrates.

where ρ_f is fluid density ($\text{kg}\cdot\text{m}^{-3}$), C_f is fluid specific heat ($\text{J kg}^{-1} \text{K}^{-1}$), A_f is fluid area, T_f is fluid temperature ($^{\circ}\text{C}$).

For Insulation in PVT

$$\rho_{ins} \delta_{ins} C_{ins} \frac{dT_{ins}}{dt} = h_{cond,ins \rightarrow tube} f_{tube,ins} (T_{tube} - T_{ins}) + f_{abs,ins} h_{cond,abs \rightarrow ins} (T_{abs} - T_{ins}) + h_w (T_{amb} - T_{ins}) \quad (15)$$

For Insulation in PVT-PCM

$$\rho_{ins} \delta_{ins} C_{ins} \frac{\partial T_{ins}}{\partial t} = h_{cond,ins \rightarrow PCM} f_{PCM,ins} (T_{PCM} - T_{ins}) + h_{cond,tube \rightarrow ins} f_{tube,ins} (T_{tube} - T_{ins}) + h_w (T_{amb} - T_{ins}) \quad (16)$$

where ρ_{ins} is insulation density ($\text{kg}\cdot\text{m}^{-3}$); δ_{ins} is insulation thickness (m); C_{ins} is insulation specific heat ($\text{J kg}^{-1} \text{K}^{-1}$); $h_{cond,ins \rightarrow tube}$ is equivalent conduction coefficient between the insulation and the tubes ($\text{Wm}^{-2} \text{K}^{-1}$); $f_{PCM,ins}$ is the contact factor of the PCM and insulation, which is

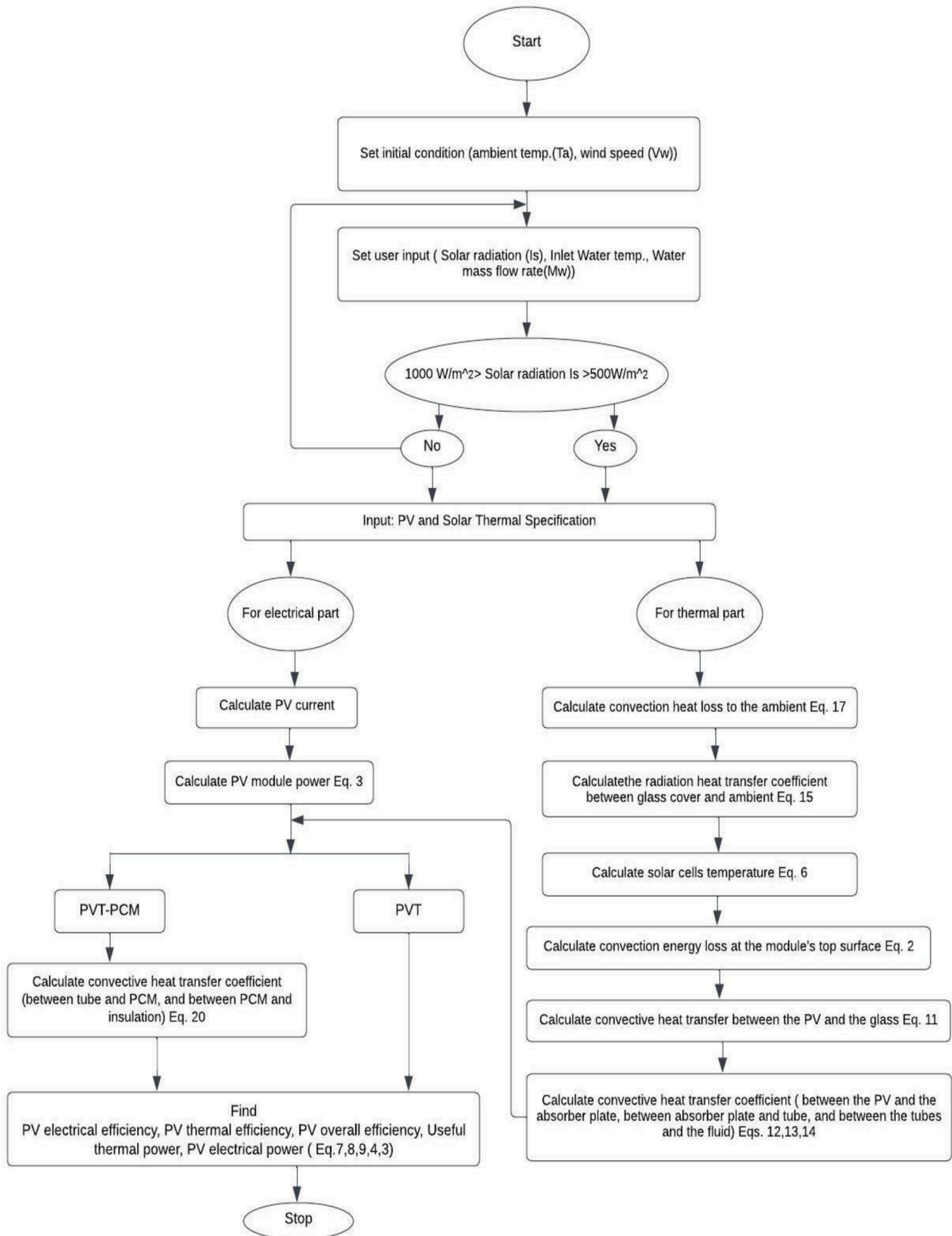


Fig. 4. Flowchart diagram of the Matlab calculation procedure.

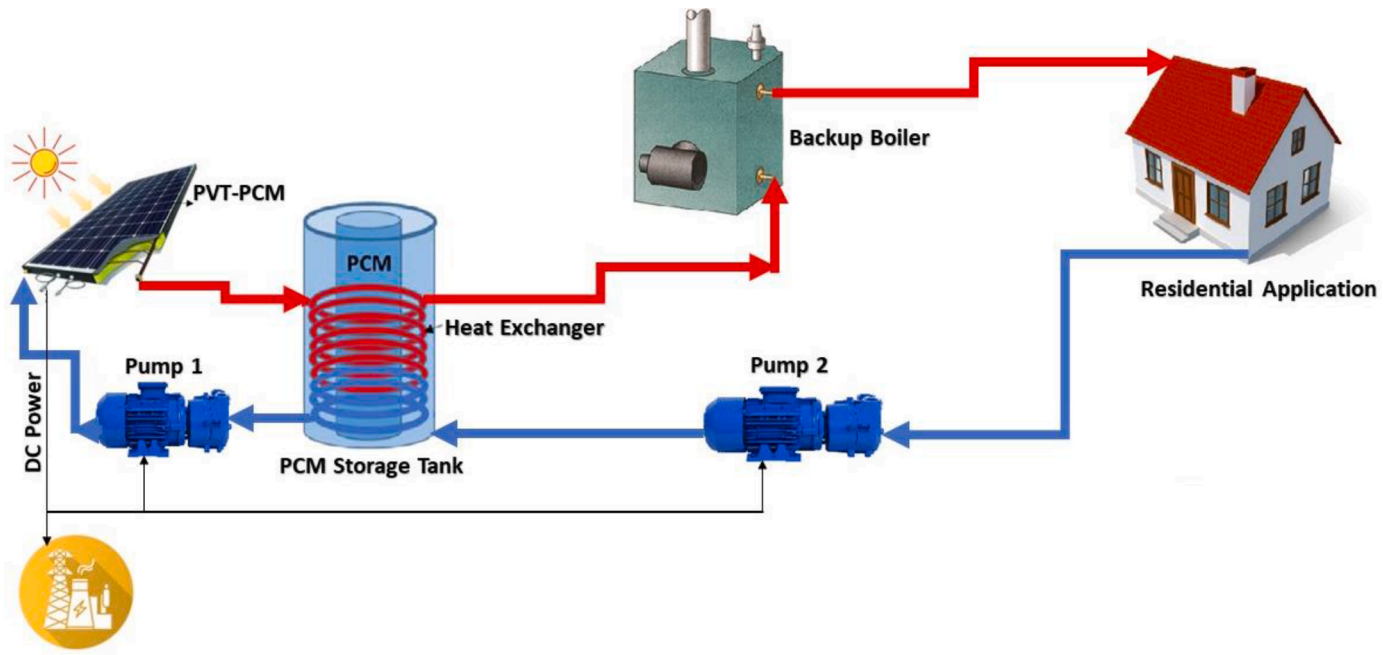


Fig. 5. Flowchart of the PVT-PCM proposed system from generation to consumption.

equal to one in contact parts or zero in noncontact; $f_{tube,ins}$ is the contact factor of the tube and insulation, which is equal to one in contact parts or zero in noncontact; $h_{cond,abs \rightarrow ins}$ is equivalent conduction coefficient between the absorber plate and the insulation ($Wm^{-2} K^{-1}$)

Heat transfer coefficients

The heat transfer coefficients in use in the computations are listed below. The irradiance heat transfer coefficient between the PV and the atmosphere is estimated as

$$h_{rad,g \rightarrow env} = \epsilon_g \sigma (T_g^2 + T_{sky}^2) (T_g + T_{sky}) \quad (17)$$

where σ is Stefan- Boltzmann constant = $5.670367 \times 10^{-8} (Wm^{-2} k^{-4})$, T_{sky} , is calculated by the following empirical equation [56]

$$T_{sky} = 0.0552 * T_{amb}^{1.5} \quad (18)$$

The wind-induced convective coefficient is defined as [57]

$$h_w = 5.7 + 3.8V_w, \text{ if } V_w < 5 \frac{m}{s}; h_w = 6.47 + V_w^{0.78}, \text{ if } V_w > 5 \frac{m}{s} \quad (19)$$

Between the fluid and the tube, the convective coefficient $h_{conv,tube \rightarrow f}$ is represented as [58]

$$Re < 2300 \Rightarrow Nu = 4.364; Re > 2300 \Rightarrow Nu = 0.023Re^{0.8} Pr^{0.4} \quad (20)$$

where Re is Reynolds number, Nu is Nusselt number, the Prandtl number (Pr) may be determined using the following formula:

$$Pr = \frac{\mu_f C_f}{k_f} \quad (21)$$

where μ_f is Dynamic viscosity of the fluid ($N.s.m^{-2}$), and k_f : Thermal conductivity ($Wm^{-1}K^{-1}$).

4. Simulation system design

The procedures used to compare and contrast thermal and electrical characteristics of the PVT systems with and without PCM are depicted in Fig. 3. The PVT-PCM model was developed employing MATLAB/Simulink to test the functionality of the proposed solar system. A flowchart diagram of the Matlab calculation procedure is displayed in Fig. 4. The flowchart of the proposed PVT-PCM system from generation to

Table 3

PVT and PVT-PCM system components' characteristics.

Components	Material	Description
PV Panel	Polycrystalline Silicon	Cell Area: 0.015 m ² Number of Cells: 36 Number of Modules: 150
Thermal Pipes	Copper	Tube Diameter: 12.7 mm Number of Tube: 25
PCM Used	Lauric Acid	Thickness: 10 mm Melting Temperature: 43.3 >°C Latent Heat: 210.8 kJ/kg
Pump	Stainless Steel	Pump Type: Centrifugal Pump Efficiency: 0.75 Pressure Drop: 1 bar
Storage Tank	Galvanized Steel Combined with PCM Material	Shape: Cylindrical

consumer is displayed in Fig. 5. The user may easily access and manage the system settings for each subsystem. Table 3 lists the specific structural parameters of each component of the system.

5. System validation

Experiments and numerical investigations have been used to verify the simulation approach for the two separate systems, PVT and PVT-PCM. The operational conditions and input parameters for both of these systems are chosen the same way as in references [59–62].

5.1. PVT system validation

The predicted outlet temperature of the collector/PVT system was subjected to both theoretical and experimental results reported by Khanjari et al. [59] and Selmi et al. [60] to validate the simulation findings.

The input solar energy in these investigations ranged from 470 to 542 W/m^2 , m_f was 0.000136 kg/s, the temperature of the inflow ranged between 32 and 46 °C., and the fluid flow was water.

The current investigation's design and operating circumstances are substantially identical to the input values. In Fig. 6(a), the collector's

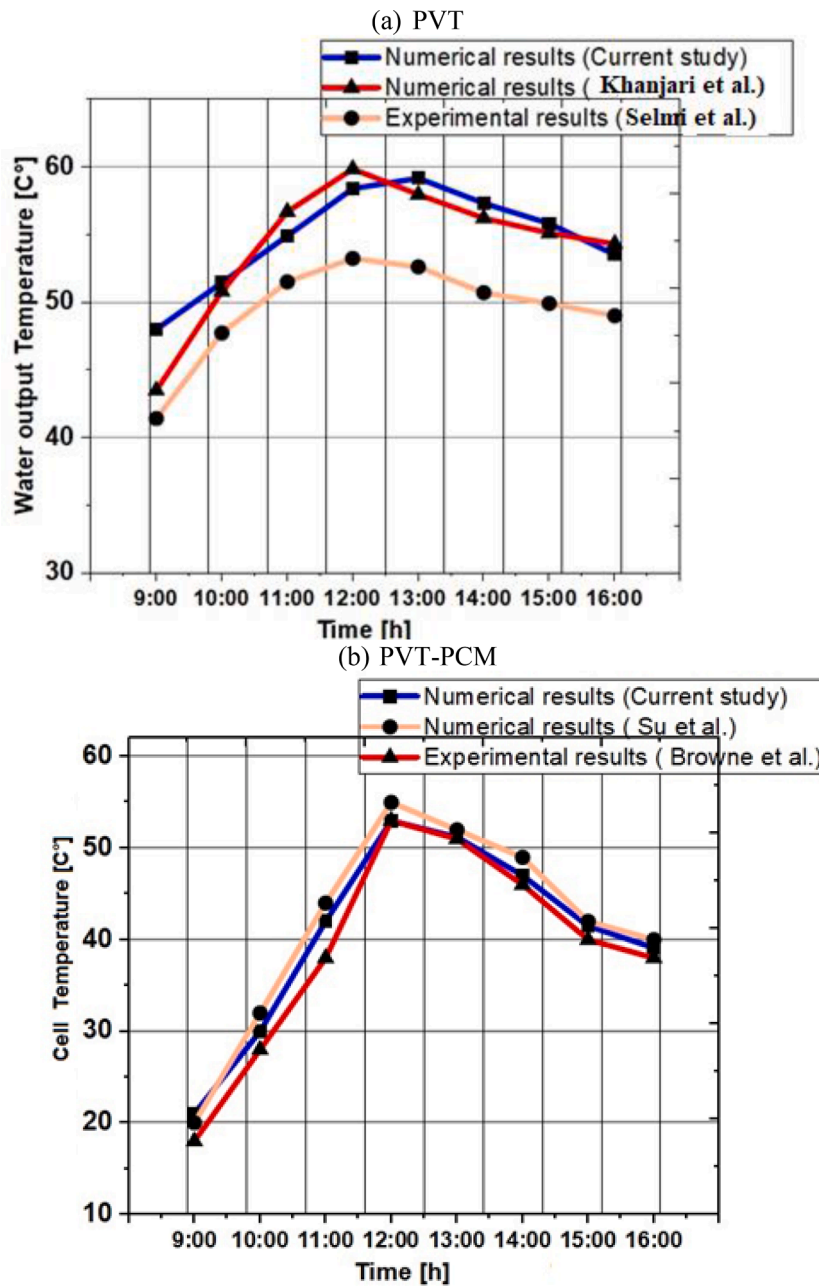


Fig. 6. Validation of a current numerical analysis with other scholars; (a) PVT configuration, (b) PVT-PCM configuration.

output temperature throughout the day is compared to the current study utilizing both numerical and experimental methods. The figure shows that the average difference between current study and the numerical analysis performed by Khanjari et al. [59], and the experimental results reported by Selmi et al. [60] is approximately 10.9% and 3.2% of the Celsius degree, respectively. The simulated PVT model, based on these observations, offers adequate accuracy and durability for all the simulations in this study.

5.2. PVT-PCM system validation

Experimental and computational studies on a PVT/PCM system were performed by Su et al. [62] and Brown et al. [61]. It is worth mentioning that the current investigation's layout and design variables are substantially identical to those of the two reference publications. All input parameters are chosen in the same way as in the references to ensure that the numerical research is valid. Fig. 6(b) shows the present study's

surface temperature as well as that in the two reference models.

Based on the acquired data, the average and lowest discrepancies among the present findings and the experimental results of Brown et al. [61] are 4.1% and 16% of the Celsius degree, respectively. Furthermore, the average and highest deviations between the ongoing findings and numerical results of Su et al. [62] are 2.75% and 6.9% of the Celsius degree, respectively, implying that the current study and other investigations are in good agreement.

6. Results and analysis

In this study, the effectiveness of PVT and PVT-PCM collectors was quantitatively examined. A new thermal collector approach was implemented by using copper as a material. The main parameters for the irradiation range of 500–1000 W/m² are considered in this research. T_{amb} and the inlet cold-water temperature to the PVT are both chosen to be 25 °C. The simulation has been used to evaluate the efficiencies of

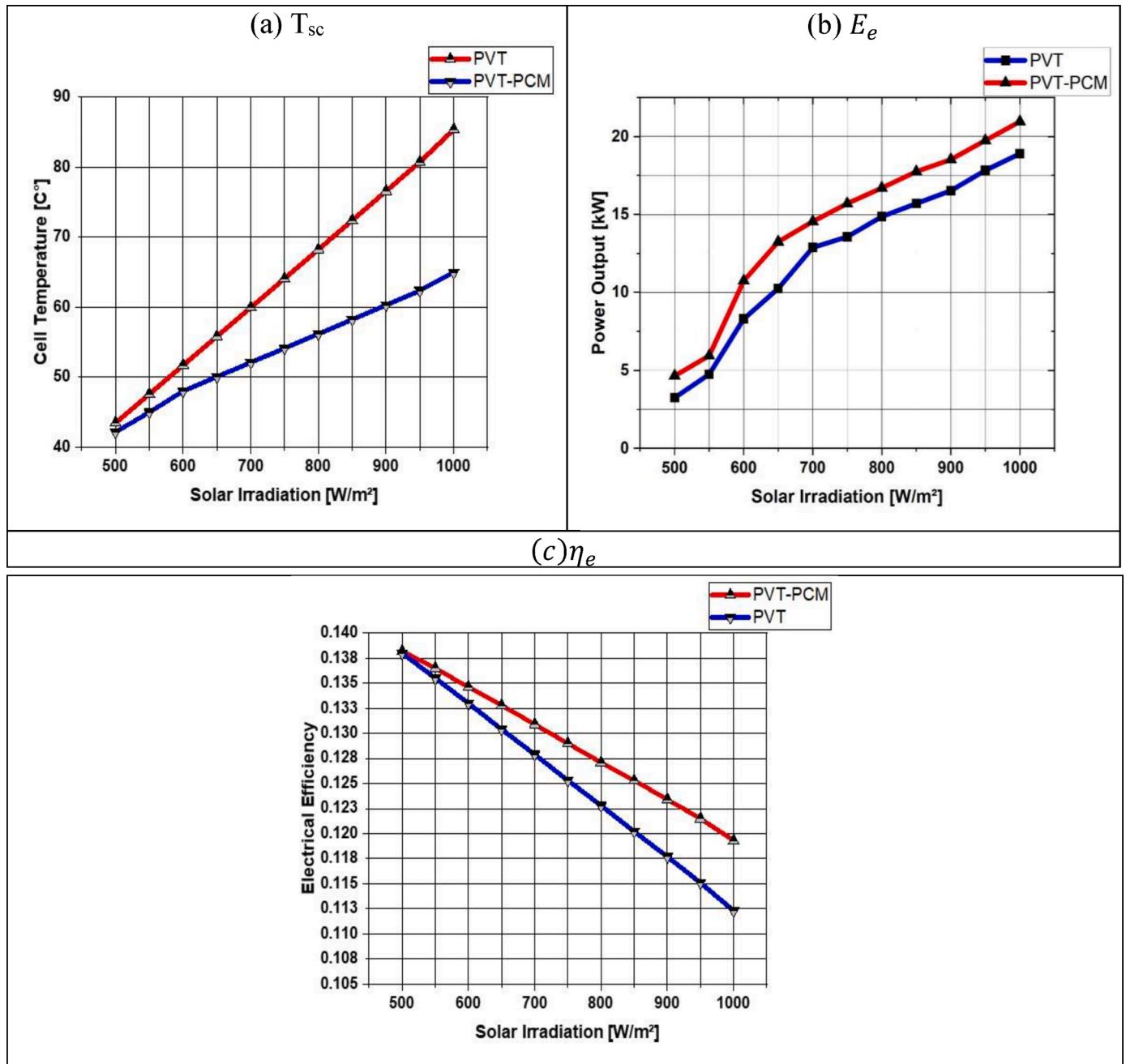


Fig. 7. Effect of solar irradiation on (a) cell temperature; (b) electrical output power, and (c) electrical efficiency for PVT and PVT-PCM configurations.

the two systems. The electrical output power, cell and water output temperatures, η_e , η_{th} , and η_o , and influence of PCM on PVT and storage tank were all factors considered in the comparison.

6.1. Electrical performance at various irradiation stages

Fig. 7 depicts the influence of incident irradiation on: (a) cell temperature (T_{sc}); (b) electrical output power (E_e); and (c) electrical efficiency (η_e) for PVT and PVT-PCM configurations. Numerically, according to Fig. 7(a), the average T_{sc} rises as the irradiation rate rises. As incident irradiance increases, the PV absorbs more heat, causing the PV cells' ambient levels to increase. The T_{amb} is 25 °C, and the inflow water temperature is 25 °C at a constant mf of 0.7 kg/s. The PVT-PCM system, as shown, has the best performance with the least amount of T_{sc} increases. Because the PCM absorbs heat latently, the T_{sc} of the PVT-PCM system is reduced. The T_{sc} of PVT reaches a high of 85.4 °C and a

low of 43.4 °C. In addition, every 50 W/m² increase results in a 4.1 °C rise in cell temperature. PVT-PCM has a lower T_{sc} than PVT, with a high of 64.9 °C and a minimum of 42.1 °C. In addition, every 50 W/m² increase results in a 2.8 °C rise in cell temperature. When the radiation exceeds 800 W/m², the variation in temperature between the PVT and PVT-PCM becomes more visible. This is because the PCM layer cools the collector through both sensible and latent heat, minimizing the impact of solar radiation on the collector.

The effect of incident irradiation on E_e is shown in Fig. 7(b). It should be noted that when the irradiation rises, E_e improves at the same rate since both voltage and current increase, but the current develops more quickly than the voltage. As a result, the voltage rises linearly with increasing irradiation intensities. The E_e of the PVT system is lower than that of the PVT-PCM system as displayed in Fig. 7(b). The PVT-PCM absorbs more heat from the T_{sc} than PVT and eliminates the excess heat, but PCM retains heat while cooling with water, resulting in superior

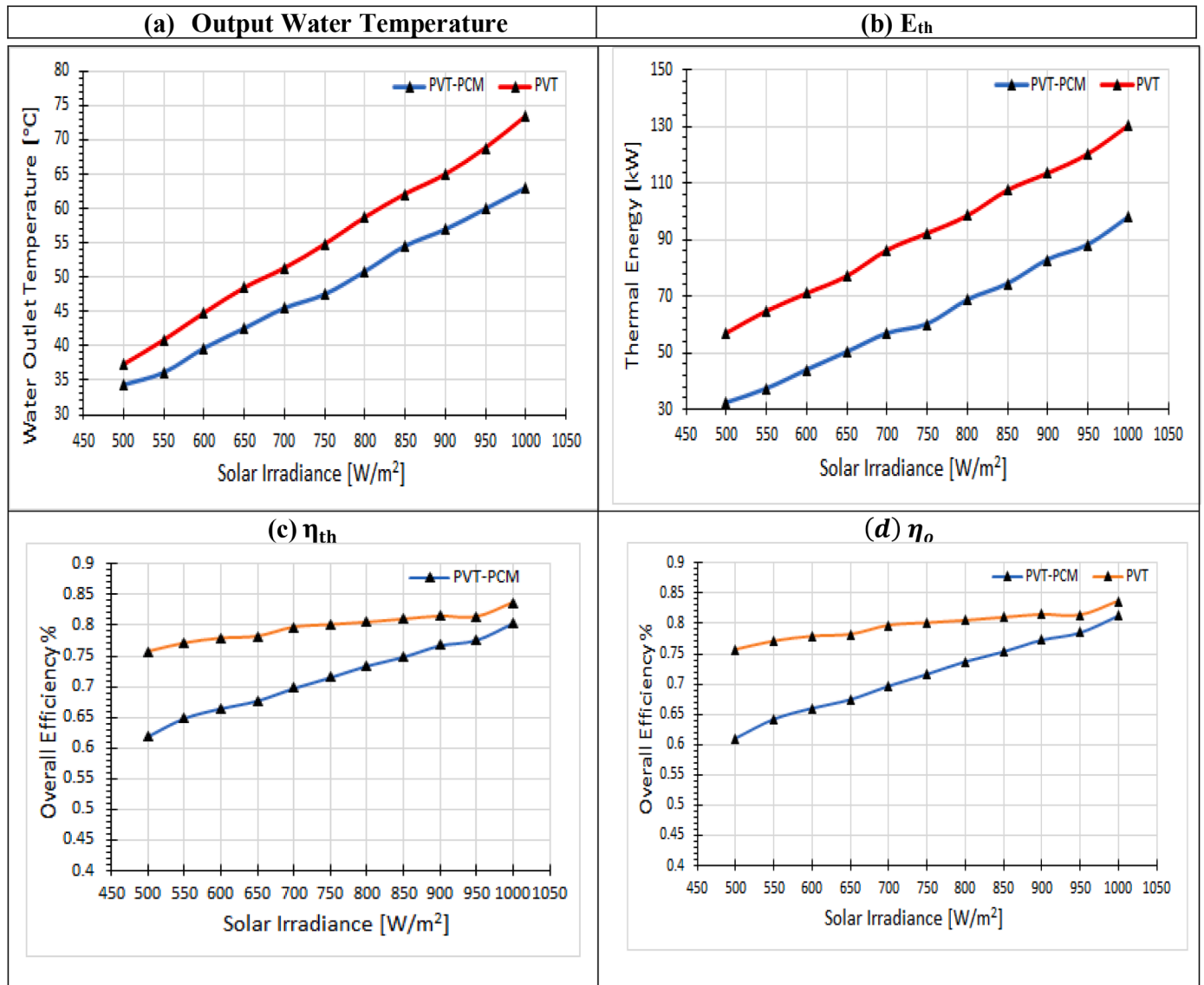


Fig. 8. Effect of solar irradiation on the (a) output temperature, (b) thermal energy (E_{th}), (c) thermal performance (η_{th}), and (d) overall efficiency (η_o) for the PVT and PVT-PCM systems.

power production.

Fig. 7(c) displays the influence of incident irradiation on electrical efficiency for PVT and PVT-PCM systems. As the incident solar radiation flux increases, the electrical efficiency of the system decreases due to the significant rise in cell temperature that occurs at high incoming radiation flux levels. The trend observed was in line with the study conducted by Fayaz et al. [63]. As shown in the figure, the η_e of the PVT configuration decreases from 13.75 to 11.1%. The η_e of the PVT-PCM configuration falls from 14% to 11.9%. Furthermore, with every 50 W/m^2 , the η_e declines by 0.17%. In contrast, the PVT is shown to have a 0.25% drop in η_e with every 50 W/m^2 .

6.2. Thermal performance at various irradiation stages

The influence of solar irradiation on (a) the output temperature, (b) thermal energy (E_{th}), (c) thermal performance (η_{th}), and overall efficiency (η_o) for the PVT and PVT-PCM systems are depicted in Fig. 8.

As the irradiation intensity grows from 500 W/m^2 to 1000 W/m^2 , the water outlet temperature rises, as illustrated in Fig. 8(a). The heat transfer rate between the PV plates and from Tedlar towards the aluminum heat exchanger by conduction and convection, and

eventually to running water, is rising because of the increased temperature gradient.

The heat transmission is accelerated by a large temperature differential. Therefore, additional energy is delivered to the working fluid at higher rates as the amount of irradiation rises. Consequently, the temperature of the industrial process rises. The rate of heat transfer remains constant from 500 W/m^2 to 1000 W/m^2 . The PVT system produces water output temperatures of 37.4 °C and 73.4 °C at 500 W/m^2 and 1000 W/m^2 , respectively. On average, the output temperature increases for PVT and PVT-PCM by 3.6 °C and 2.8 °C for every 50 W/m^2 increase, respectively. The water output temperature for PVT-PCM is 34.3 °C and 62.99 °C at 500 W/m^2 and 1000 W/m^2 , respectively.

The E_{th} interaction with solar irradiation in the range of 500–1000 W/m^2 is depicted in Fig. 8(b). When the temperature differential affected by excessive solar irradiation is significant, the amount of heat transferred from the thermal collector to the water grows dramatically. Consequently, 1000 W/m^2 produces more E_{th} than 500 W/m^2 due to enhanced heat transfer mechanisms inside the system. The highest E_{th} value for the PVT system is 130.6 kW at 1000 W/m^2 . At 500 W/m^2 , a minimum E_{th} value of 57 kW is attained. Thermal energy is achieved at an average of 7.3 W per 50 W/m^2 irradiation. Similarly, the highest E_{th}

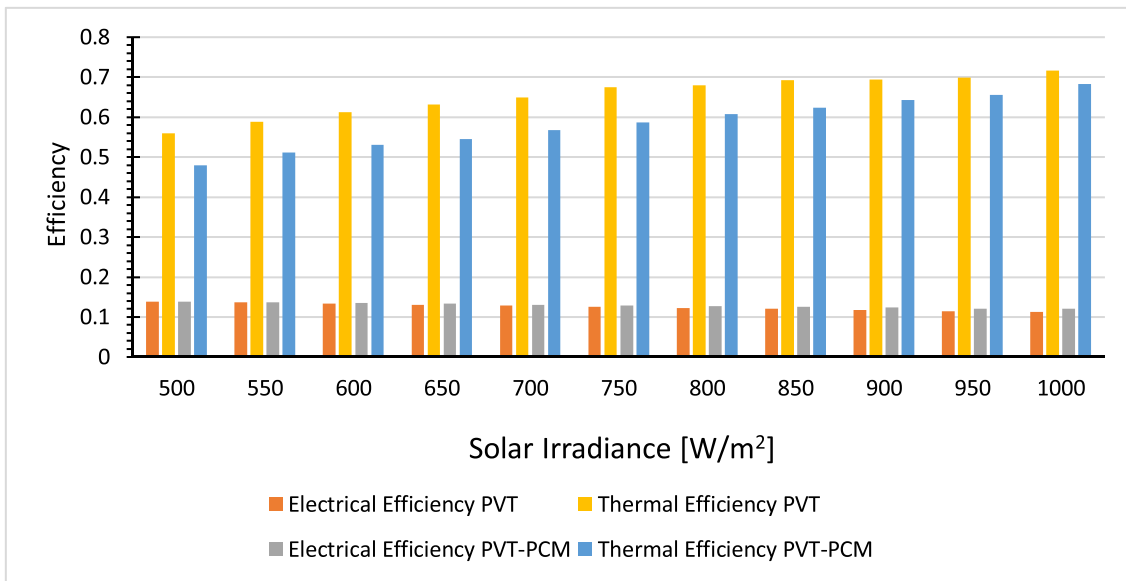


Fig. 9. Electrical and thermal efficiency comparison performance of PVT and PVT-PCM for different solar irradiation.

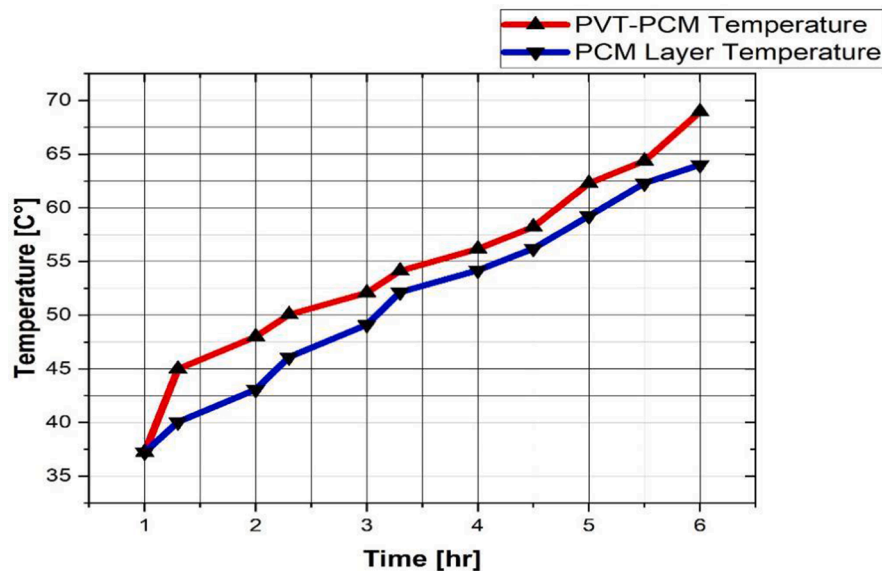


Fig. 10. Temperatures of the cell and PCM layer in the PVT-PCM.

obtained by PVT-PCM at 1000 W/m² is 97.88 kW.

Fig. 8(c) displays the thermal efficiency of both systems within the solar irradiation range of 500 W/m² to 1000 W/m². The PVT system reaches a maximum η_{th} of 71.7% at 1000 W/m². At 500 W/m², the lowest η_{th} is 56.1%. On average, for every 50 W/m², the η_{th} rises by 0.8%. The PVT-PCM has a η_{th} of 68.4% at 1000 W/m². The minimum η_{th} is 48.1% at 500 W/m². For every 50 W/m², the η_{th} rises by 2.03% on average. When PCM is integrated into PVT, the E_{th} and η_{th} decrease because some of this energy is stored in the PCM layer to be used at a later time, such as at night or when the PV is in shadow.

Fig. 8(d) displays the total efficiency of the systems as a function of solar irradiation. The sum of η_e and η_{th} gives the overall efficiency (η_o), with the latter accounting for the bulk of the variation in η_o with changing solar irradiation. The η_o of the PVT system at maximum values is 83.7% at 1000 W/m². The lowest η_o is 75.7% at 500 W/m². The PVT-PCM system has the lowest η_o of 61.9% at 500 W/m² and the maximum η_o of 80.35% at 1000 W/m².

6.3. Evaluation of comparative performance at various irradiation stages

The performance of a PVT-PCM system has been compared to the performance of a PVT system. Fig. 9 shows the performance of the PVT-PCM system and that of the PVT, revealing that the η_e of the PVT-PCM increased by 2.97% compared to the PVT systems, while the η_{th} of the PVT-PCM decreased by 10.63% compared to the PVT system. The drop in E_{th} in the PVT-PCM system is due to the PCM storing a considerable portion of this energy for usage when solar radiation is not available. This study exhibited outcomes consistent with Fayaz et al. [63].

6.4. Effect of PCM on PVT and storage tank

Fig. 10 depicts the temperature variation of the PV module and PCM layer in the PVT-PCM, showing the temperature progression of the PV module and PCM layer over a six-hour period. The results demonstrate that the temperature of the PVT-PCM layer increased from 37 °C to 67 °C, while that of the PCM layer increased from 35 °C to 64 °C, and both

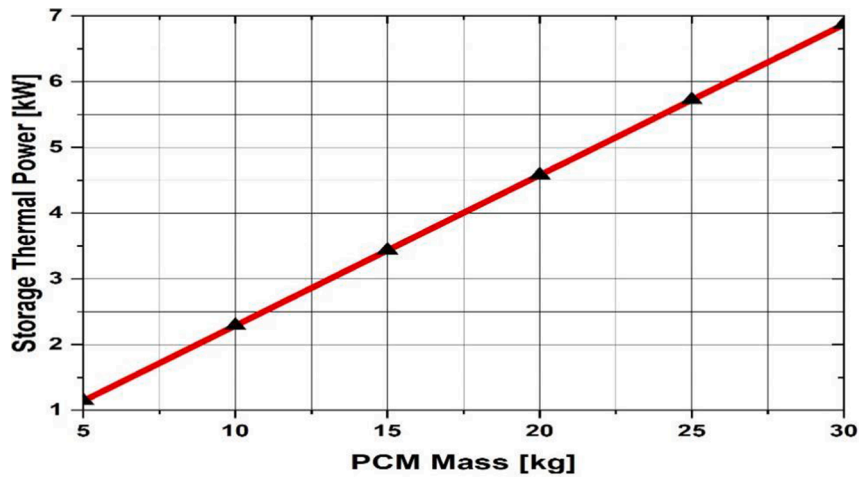


Fig. 11. Effect of mass of PCM on the thermal energy stored in the storage tank.

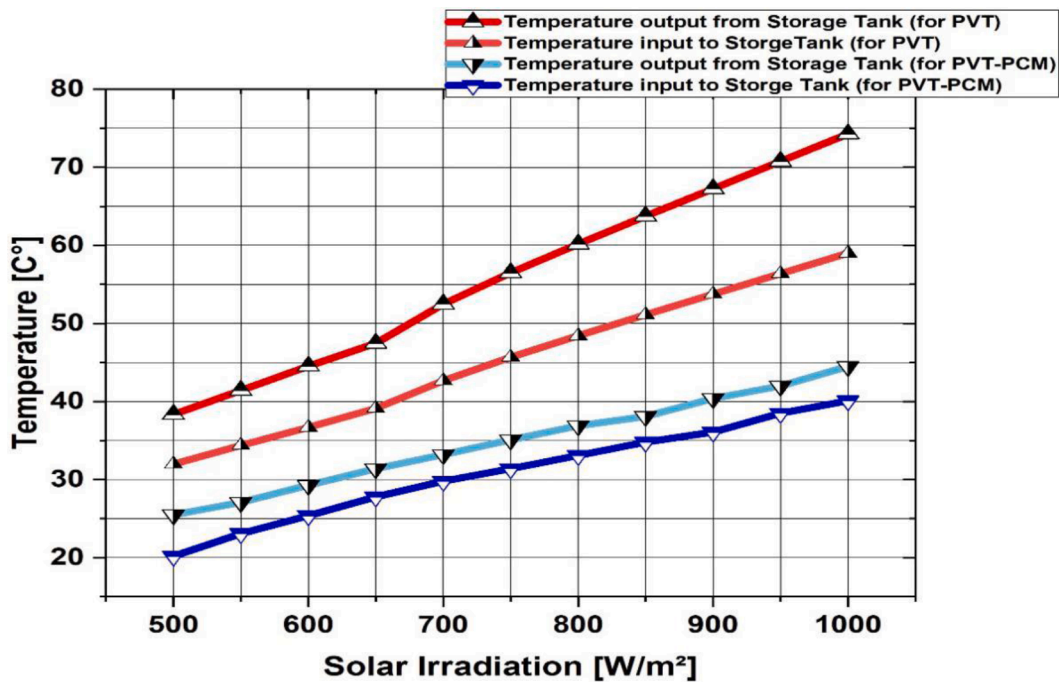


Fig. 12. Effect of solar irradiation on the temperatures of output and input in the storage tank.

followed a similar pattern. Lauric acid was used to store latent heat energy. At 36 °C, the PCM layer was in the solid phase. Consequently, during the rapid rise in temperatures of the cell and PCM layer in response to the solar radiation, the PCM absorbed thermal energy and cooled the cell significantly.

Fig. 11 represents the effect of the mass of PCM on the amount of Eth stored in the storage tank.

The results show a linear relationship between the PCM mass and the stored energy, resulting in an increase in the amount of energy stored as the mass of PCM increases from 5 to 30 kg. This increase in stored energy improves the efficiency of the storage tank in retaining heat, which is reflected in the system's power, which can reach up to 7 kW.

Fig. 12 demonstrates the variations in output and input temperatures in the storage tank of the PVT and PVT-PCM systems with solar irradiation ranging from 500 W/m² to 1000 W/m². As a result, as the intensity of the irradiation increases, the temperatures of the output and input in the storage tank increase. The PVT system's output and input

temperatures in the storage tank are greater than for the PVT-PCM system. The drop in temperatures in the PVT-PCM system is due to the PCM absorbing a considerable portion of the energy, resulting in lower temperatures than in the PVT system.

6.5. Impact of mass flow rate on the electrical and thermal output of PVT and PVT-PCM

Fig. 13(a) shows the effect of mass flow rates on the cell temperature. As shown in Fig. 13(a), the mean temperature of the cell drops as the mass flow rate (\dot{m}) rises. Surplus heat is transmitted to flowing water via convection when the inflow \dot{m} is increased, resulting in a fall in T_{sc} . There is a considerable decline in T_{sc} when the \dot{m} increased from 0.7 kg/s to 0.95 kg/s. The largest quantity of heat is lost because of a large temperature difference since the T_{sc} is greater and the inflow \dot{m} is lower. There is a considerable difference in T_{sc} reductions between the two systems. This distinction is drawn because the PCM retains more

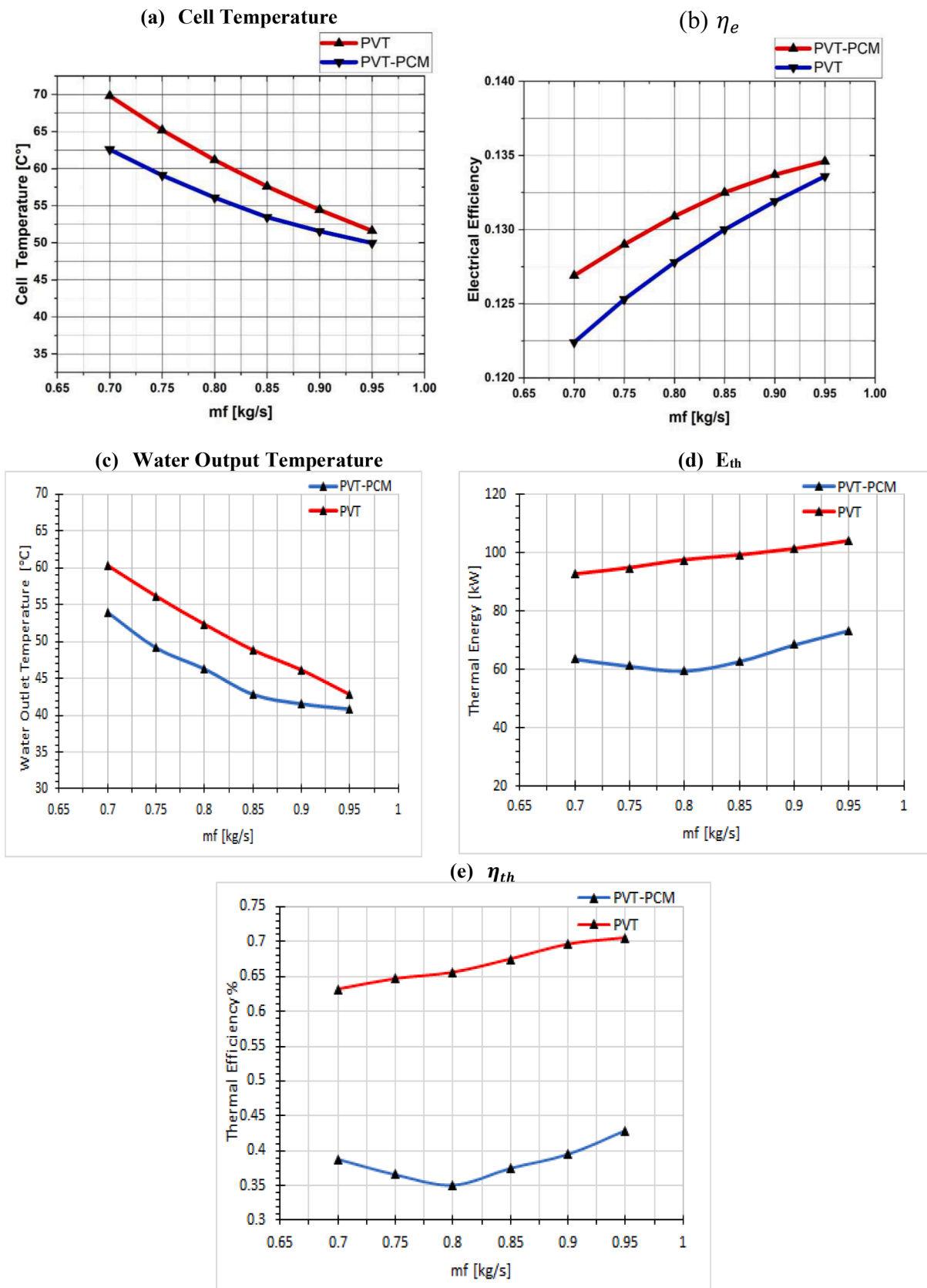


Fig. 13. Mass flow rate effect on (a) cell temperature; (b) electrical efficiency; (c) water output temperature; (d) thermal energy; and (e) thermal efficiency for the PVT and PVT-PCM systems.

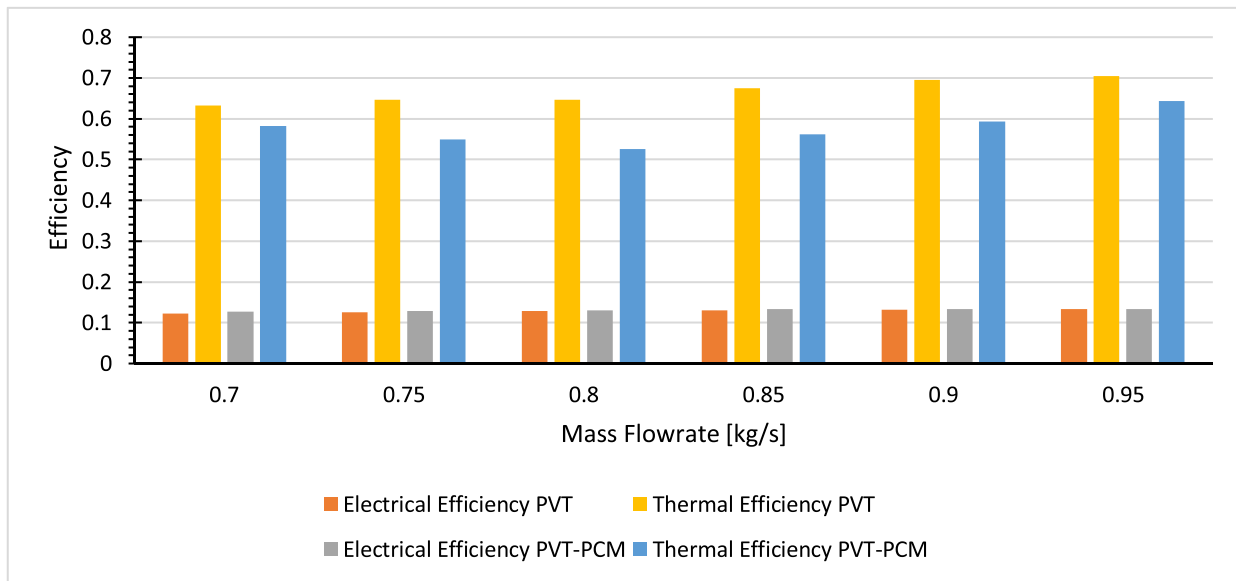


Fig. 14. Electrical and thermal efficiency comparison performance of PVT and PVT-PCM for different mass flow rates.

heat from the cell concurrently with the PVT system, hence the PCM removes the most heat. The maximum T_{sc} for PVT is 74.6 °C, whereas the greatest T_{sc} for PVT-PCM is 69.1 °C, as shown in Fig. 13(a).

The effect of mass flow rate on electrical efficiency is depicted in Fig. 13(b). In a PVT system, increasing the mass flow rate can increase the electrical efficiency by improving the cooling of the photovoltaic cells. Higher mass flow rates lower the T_{sc} dramatically. As a result, the PV voltage increases while the current decreases, boosting η_e and the output capacity of the PVT system. In other words, the increased flow rate helps to remove excess heat from the cells, which reduces the cell temperature and improves their performance. However, increasing the flow rate too much can lead to a higher pressure drop and pumping power requirements, which can reduce the overall system efficiency. The PVT-PCM has a higher η_e than the PVT system due to the greater cooling effect. η_e is around 13.5%, with a minimum η_e of 12.7%. Furthermore, the increase in η_e for every 0.1 kg/s increase is 0.4%. The findings were in agreement with the study conducted by Pang et al. [64].

Fig. 13 (c & d) depicts the outlet water temperature thermal energy versus different mass flow rates for the PVT and PVT-PCM. The temperature of the output water reduces when mf is raised, as seen in Fig. 13 (c). Low mass flow rates result in a higher water generation temperature due to more heat occupying the limited mass of water. Conversely, an increase in mass flow rate causes a decrease in output temperature because a larger mass of water accumulates more heat at a lower temperature. This behavior is because a low mass absorbs a given amount of heat at a higher temperature than a larger mass. In PVT-PCM systems, the high thermal storage capacity of PCM materials is the cause of the low output water temperature. However, this capacity presents a significant advantage for prolonged heat availability. Therefore, PVT-PCM systems are an excellent choice for supplying thermal energy during nighttime hours. As a result, the flow rate should be kept between 0.70 and 0.80 kg/s in order to maintain a warm water source for improved heat quality. The interaction of thermal energy with various mass flow rates is depicted in Fig. 13(d), with the highest E_{th} value for the PVT system being 103.1 kW. The minimum E_{th} value was 92.4 kW at 0.7 kg/s. In the case of the PVT-PCM system, the highest and lowest E_{th} values of 73.4 kW and 59.6 kW were recorded at mass flow rates of 0.95 kg/s and 0.8 kg/s, respectively.

Fig. 13(e) shows the thermal efficiency variation when mf changes from 0.70 kg/s to 0.95 kg/s for both the PVT and PVT-PCM systems. At 0.95 kg/s, the PVT and PVT-PCM systems achieve a maximum η_{th} of 70.8% and 42.7%, respectively. The lowest η_{th} is 63.2% at 0.70 kg/s

for the PVT system and 35.8% at 0.80 kg/s for the PVT-PCM system. For every 0.1 kg/s increase in flow rate, the PVT system experiences a 3% increase in η_{th} while the PVT-PCM system experiences a 5.2% increase. The PVT-PCM system has a lower thermal efficiency compared to the PVT system due to the large thermal storage capacity provided by the PCM material. This results in a longer heat availability duration but at a lower temperature, which leads to a lower overall efficiency. Furthermore, the reduced thermal efficiency of the PVT-PCM system in comparison to the PVT system could be attributed to the thermal resistance introduced by the PCM layer. This additional resistance can lower the rate of heat transfer between the PVT panel and the heat storage medium. Moreover, the melting and solidification of the PCM can cause temperature fluctuations, potentially leading to a decrease in the overall efficiency of the system. The results were consistent with the study carried out by Fayaz et al. [63].

6.6. Evaluation of comparative performance at various mass flow rates

The effectiveness of a PVT-PCM system has been compared to the effectiveness of a PVT for different mass flow rates. Fig. 14 depicts the PVT-PCM system's performance in comparison to the PVT system's performance, showing a small improvement of η_e of the PVT-PCM of about 2–4% and a reduction in η_{th} of 8–18% in comparison with the PVT configuration. The trend was consistent that observed by other scholars [65].

Table 4 provides an overview of several studies that have been conducted on PVT and PVT-PCM systems for different applications. These systems have been evaluated in a variety of weather and operating circumstances, which have a substantial influence on their performance. As depicted in the table, the electrical or thermal efficiency values differ widely among the different systems evaluated in different environments. Thus, comparing systems with different designs and configurations operating under varying weather conditions can be challenging. Nonetheless, each system has demonstrated a significant improvement in performance. Our current study has successfully increased the electrical power output of a PV module by up to 14% under the weather conditions of Amman, Jordan. It is worth mentioning that the electrical efficiency of our proposed system is among the highest compared to other systems presented in Table 4. However, several factors, such as PV technology, location, system configuration, thermal system type, and cooling methods, can impact the results.

Table 4
A Comparative performance analysis of the current study and the literature.

Reference	System Configuration	Thermal Efficiency (%)	Electrical Efficiency (%)	Remarks
Alzaabi et al. (2014) [20]	PVT	60% to 70%	–	-In the climate conditions of Sharjah, UAE - Compared to a PV panel, the PV/T system shows an increase in electrical power output by 15 to 20%.
Liang et al. (2015) [23]	PVT	–	7.2%	- PVT solar collector filled with graphite
Wu et al. (2011) [25]	heat pipe PVT	63.65%	8.45%	The range of operating temperatures for solar cells on a solar PV panel varies by less than 2.5 °C.
Yang et al. (2018) [27]	PVT and PVT-PCM	58.35 and 70.34	6.98 and 8.16	The total conversion efficiency of solar energy is 63.93% for the PVT system and 76.87% for the PVT-PCM system.
Ahmadi et al. (2021) [29]	PV-PCM + water cooler PV- PCM-composite + water cooler]	13 and 13.2	40 and 54	The addition of PCM reduced the temperature of the PV-cell by up to 6.8% (around 4 °C) and increase the electrical efficiency by up to 14%.
Gaur et al. (2017) [35]	PVT and PVT-PCM	16.5% and 16.87% for winter 15.4% and 16.3% for summer	33 and 38 for winter; 22 and 22 for summer	In Lyon, France, PCM incorporation in the PVT system led to a significant reduction in module temperature during summer and winter days. The maximum temperature reduction observed was approximately 16.04 °C at 12 PM during summer and approximately 5 °C at 1 PM during winter.
Hossain et al. (2023) [36]	PVT and PVT-PCM	75.29 and 86.19	10.56 and 11.51	Under climate of Malaysia, the utilization of PCMs resulted in an increase in the performance of both electrical and thermal aspects of PV systems.
Fayaz et al. (2019) [65]	PVT and PVT-PCM	74% and 65%	9.2 and 12.75%	Kuala Lumpur, Malaysia.
Hossain et al. (2019) [66]	PV and PVT	74.62 for PVT	9.88 and 10.46	Under climate of Malaysia, the electrical efficiency of PV/T systems was found to be enhanced by 5.76%

Table 4 (continued)

Reference	System Configuration	Thermal Efficiency (%)	Electrical Efficiency (%)	Remarks
Al-Waeli et al. (2017) [67]	PVT, PVT-PCM PVT-nano PCM	35.4, 50.5, and 72	9.92, 9.92, and 13.70	compared to PV systems. By using nanofluid as a coolant for a PV/T system, the thermal energy obtained from photovoltaic cells were increased.
Current Study	PVT and PVT-PCM	70.8% and 64.5%	13.75% and 14%	Under the weather conditions of Amman, Jordan Investigated the effect of mass flow rate on the electrical and thermal output of PVT and PVT-PCM systems

7. Study limitations

This study provides valuable insights into the application of phase change material on the performance of photovoltaic thermal systems. However, it is important to note that this study is hindered by three significant limitations that must be addressed in future research. The first limitation is that the assumptions underlying the mathematical model used to simulate the PVT system may not fully represent the actual behavior of the system in the field. For example, the assumption of a dust-free PV surface may not be valid in practice, which could impact the efficiency of the system. The second limitation is that the study only examines the impact of PCM on PVT systems with copper pipe. The results may not be applicable to other types of PVT systems. Finally, the study does not investigate the long-term durability of the PCM material or the impact of thermal cycling on its performance.

To address the first limitation, future research could focus on validating the assumptions made in the mathematical model by conducting experiments under real-life conditions. This would involve measuring the impact of dust and other factors that may affect the system's performance and PV efficiency. To overcome the second limitation, future studies could investigate the impact of PCM on PVT systems with different types of cooling systems. This would provide a more comprehensive understanding of how PCM can improve the performance of PVT systems. Finally, to address the third limitation, future research could explore the long-term durability of the PCM material and its performance under different environmental conditions. This would help identify any potential issues with using PCM in PVT systems over extended periods and inform the development of more reliable and durable PCM materials.

8. Conclusion

This study examined the performance of PVT and PVT-PCM systems employing copper pipe using numerical analysis in MATLAB. Although there have been studies on the impact of PCM on PVT systems, there is still a need to investigate the effect of PCM on thermal energy storage, and the electrical and thermal efficiency of PVT-PCM systems. The study investigated the thermal and electrical efficiencies of the PVT-PCM system and compared it with those of a conventional PVT system without PCM, under the weather conditions of Amman, Jordan. Furthermore, the study aimed to investigate the impact of coolant mass flow rate and solar irradiation on the solar cell temperature, water output temperature, electrical and thermal output and efficiencies of PVT and PVT-PCM systems. The following are the key findings of this

study:

- Compared to the PVT system without PCM, the PVT system with PCM was capable of lowering cell temperatures by 24% (up to 19 °C) and enhancing electrical efficiency by 5.9%.
- The electrical efficiency of both the PVT and PVT-PCM systems could be enhanced by increasing the mass flow rate, which improves the cooling of the photovoltaic cells. Higher mass flow rates considerably decrease the temperature of the solar cell, leading to an increase in PV voltage while the current reduces. Consequently, the electrical efficiency and output capacity of the system are boosted.
- The solar cells in the PVT system experience temperatures ranging from 43.44 °C to 85.4 °C, with variations in irradiance causing a 4.1 °C increase for every 50 W/m² increment. The PVT-PCM system has a maximum cell temperature of 64.9 °C and a minimum of 42.1 °C, with a 50 W/m² increase in irradiance leading to a 2.8 °C rise in cell temperature.
- The inclusion of a PCM in the PVT system resulted in a negative impact on both the thermal energy and thermal efficiency, causing an average reduction of 32.18% and 10.63%, respectively. The reduction in thermal energy and thermal efficiency can be attributed to the significant thermal storage capacity offered by the PCM material. This capacity prolongs the availability of heat but at a reduced temperature, thereby decreasing the overall efficiency.
- On average, the water output temperatures of the PVT-PCM system were observed to be 6.8 >°C and 5.3 >°C lower than that of the PVT system, under varying solar irradiance and mass flow rates, respectively.
- 1000 W of solar irradiation produced the maximum overall efficiency for both the PVT and PVT-PCM systems, 83.3% and 80.35%, respectively. Similarly, the highest thermal efficiency for the PVT and PVT-PCM systems were 71.7% and 68.35%, respectively, at the same solar irradiation level.

In the future, the following areas will be examined in depth:

- Investigate the impact of different types of PCMs on the performance of PVT-PCM systems.
- Study the effect of varying the PCM thickness on the performance of PVT-PCM systems.
- Conduct experimental studies to validate the numerical analysis results obtained in this study. This can provide more accurate data and help confirm the reliability of the simulation model.

The results of this study provide valuable insights for future research and the design of PVT-PCM systems. The findings of this study can contribute to the development of more efficient and sustainable solar energy systems by identifying ways to further improve the performance of PVT-PCM systems.

Declaration of Competing Interest

The authors declare no conflict of interest.

The authors declare that they have no known competing financial interests or personal relationships that could have appeared to influence the work reported in this paper.

The authors declare the following financial interests/personal relationships which may be considered as potential competing interests.

Data availability

No data was used for the research described in the article.

References

- [1] M.R. Gomaa, M. Al-Dhaifallah, A. Alahmer, H. Rezk, Design, modeling, and experimental investigation of active water cooling concentrating photovoltaic system, *Sustainability* 12 (2020) 5392.
- [2] N. Khordehgah, V. Guichet, S.P. Lester, H. Jouhara, Computational study and experimental validation of a solar photovoltaics and thermal technology, *Renew. Energy*. 143 (2019) 1348–1356.
- [3] A. Alahmer, M. Al-Dabbas, S. Alsaqoor, A. Al-Sarayreh, Utilizing of solar energy for extracting freshwater from atmospheric air, *Appl. Sol. Energy*. 54 (2018) 110–118.
- [4] A. Alahmer, S. Alsaqoor, Energy efficient of using chilled water system for sustainable health care facility operating by solar photovoltaic technology, *Energy Procedia* 156 (2019) 65–71.
- [5] M.I. Al-Amayreh, A. Alahmer, A. Manasrah, A novel parabolic solar dish design for a hybrid solar lighting-thermal applications, *Energy Reports* 6 (2020) 1136–1143.
- [6] O. Badran, A. Alahmer, F.A. Hamad, Y. El-Tous, G. Al-Marahle, H.M.A. Al-Ahmadi, Enhancement of solar distiller performance by photovoltaic heating system, *Int. J. Thermofluids*. 18 (2023), 100315, <https://doi.org/10.1016/j.ijft.2023.100315>.
- [7] A. Alahmer, S. Ajib, Solar cooling technologies: state of art and perspectives, *Energy Convers. Manag.* 214 (2020), 112896.
- [8] M. Song, F. Niu, N. Mao, Y. Hu, S. Deng, Review on building energy performance improvement using phase change materials, *Energy Build.* 158 (2018) 776–793.
- [9] M.I. Al-Amayreh, A. Alahmer, Design a solar harvester system capturing light and thermal energy coupled with a novel direct thermal energy storage and nanoparticles, *Int. J. Thermofluids*. (2023), 100328.
- [10] J. Luo, D. Zou, Y. Wang, S. Wang, L. Huang, Battery thermal management systems (BTMs) based on phase change material (PCM): a comprehensive review, *Chem. Eng. J.* 430 (2022), 132741.
- [11] Y.-C. Weng, H.-P. Cho, C.-C. Chang, S.-L. Chen, Heat pipe with PCM for electronic cooling, *Appl. Energy*. 88 (2011) 1825–1833.
- [12] A. Afzal, C.A. Saleel, I.A. Badruddin, T.M.Y. Khan, S. Kamangar, Z. Mallick, O. D. Samuel, M.E.M. Soudagar, Human thermal comfort in passenger vehicles using an organic phase change material—an experimental investigation, neural network modelling, and optimization, *Build. Environ.* 180 (2020), 107012.
- [13] S. Tong, B. Nie, Z. Li, C. Li, B. Zou, L. Jiang, Y. Jin, Y. Ding, A phase change material (PCM) based passively cooled container for integrated road-rail cold chain transportation—an experimental study, *Appl. Therm. Eng.* 195 (2021), 117204.
- [14] A. Alahmer, S. Ajib, X. Wang, Comprehensive strategies for performance improvement of adsorption air conditioning systems: a review, *Renew. Sustain. Energy Rev.* 99 (2019) 138–158.
- [15] M.I. Al-Amayreh, A. Alahmer, On improving the efficiency of hybrid solar lighting and thermal system using dual-axis solar tracking system, *Energy Reports* 8 (2022) 841–847.
- [16] D. Dewangan, J.P. Ekka, T.V. Arjunan, Solar photovoltaic thermal system: a comprehensive review on recent design and development, applications and future prospects in research, *Int. J. Ambient Energy*. (2022) 1–25.
- [17] A. Hasan, S.J. McCormack, M.J. Huang, B. Norton, Evaluation of phase change materials for thermal regulation enhancement of building integrated photovoltaics, *Sol. Energy*. 84 (2010) 1601–1612.
- [18] L.P. Tan, Passive cooling of concentrated solar cells using phase change material thermal storage, (2013).
- [19] S. Preet, B. Bhushan, T. Mahajan, Experimental investigation of water based photovoltaic/thermal (PV/T) system with and without phase change material (PCM), *Sol. Energy*. 155 (2017) 1104–1120.
- [20] A.A. Alzaabi, N.K. Badawiyeh, H.O. Hantoush, A.K. Hamid, Electrical/thermal performance of hybrid PV/T system in Sharjah, UAE, *Int. J. Smart Grid Clean Energy*. 3 (2014) 385–389.
- [21] A. Naseer, F. Jamil, H.M. Ali, A. Ejaz, S. Khushnood, T. Ambreen, M.S. Khan, M. A. Bashir, W. Pao, W.M. Yan, Role of phase change materials thickness for photovoltaic thermal management, *Sustain. Energy Technol. Assessments*. 49 (2022), 101719.
- [22] I. Nardi, D. Ambrosini, T. de Rubeis, D. Paoletti, M. Muttillio, S. Sfarra, Energetic performance analysis of a commercial water-based photovoltaic thermal system (PV/T) under summer conditions, *J. Phys. Conf. Ser.* (2017) 12040.
- [23] R. Liang, J. Zhang, L. Ma, Y. Li, Performance evaluation of new type hybrid photovoltaic/thermal solar collector by experimental study, *Appl. Therm. Eng.* 75 (2015) 487–492.
- [24] H.A. Zondag, D.W. De Vries, W.G.J. Van Helden, R.J.C. Van Zolingen, A.A. Van Steenhoven, The yield of different combined PV-thermal collector designs, *Sol. Energy*. 74 (2003) 253–269.
- [25] S.-Y. Wu, Q.-L. Zhang, L. Xiao, F.-H. Guo, A heat pipe photovoltaic/thermal (PV/T) hybrid system and its performance evaluation, *Energy Build* 43 (2011) 3558–3567.
- [26] A. Hassan, H. Nouman, A. Assi, B. Norton, Temperature regulation and thermal energy storage potential of phase change materials layer contained at the back of a building integrated photovoltaic panel, in: *Proc. 30th Int. Plea Conf*, 2014, pp. 16–18.
- [27] X. Yang, L. Sun, Y. Yuan, X. Zhao, X. Cao, Experimental investigation on performance comparison of PV/T-PCM system and PV/T system, *Renew. Energy*. 119 (2018) 152–159.
- [28] M.C. Browne, K. Lawlor, A. Kelly, B. Norton, S.J. Mc Cormack, Indoor characterisation of a photovoltaic/thermal phase change material system, *Energy Procedia* 70 (2015) 163–171.
- [29] R. Ahmadi, F. Monadinia, M. Maleki, Passive/active photovoltaic-thermal (PVT) system implementing infiltrated phase change material (PCM) in PS-CNT foam, *Sol. Energy Mater. Sol. Cells* 222 (2021), 110942.

- [30] G. Dogkas, M.K. Koukou, J. Konstantaras, C. Pagkalos, K. Lymperis, V. Stathopoulos, L. Coelho, A. Rebola, M.G. Vrachopoulos, Investigating the performance of a thermal energy storage unit with paraffin as phase change material, targeting buildings' cooling needs: an experimental approach, *Int. J. Thermofluids* 3 (2020), 100027.
- [31] G. Righetti, L. Doretti, C. Zilio, G.A. Longo, S. Mancin, Experimental investigation of phase change of medium/high temperature paraffin wax embedded in 3D periodic structure, *Int. J. Thermofluids* 5 (2020), 100035.
- [32] C.S. Malvi, D.W. Dixon-Hardy, R. Crook, Energy balance model of combined photovoltaic solar-thermal system incorporating phase change material, *Sol. Energy*. 85 (2011) 1440–1446.
- [33] S.S. Bhakre, P.D. Sawarkar, V.R. Kalamkar, Numerical study on photovoltaic thermal phase change material system in hot climatic conditions, *Appl. Therm. Eng.* (2023), 120423.
- [34] M. Abd El-Hamid, G. Wei, L. Cui, C. Xu, X. Du, Three-dimensional heat transfer studies of glazed and unglazed Photovoltaic/Thermal systems embedded with phase change materials, *Appl. Therm. Eng.* 208 (2022), 118222.
- [35] A. Gaur, C. Ménéz, S. Giroux, Numerical studies on thermal and electrical performance of a fully wetted absorber PVT collector with PCM as a storage medium, *Renew. Energy* 109 (2017) 168–187.
- [36] M.D.S. Hossain, L. Kumar, A. Arshad, J. Selvaraj, A.K. Pandey, N.A. Rahim, A comparative investigation on solar PVT-and PVT-PCM-based collector constancy performance, *energies*. 16 (2023) 2224.
- [37] M. Jurčević, S. Nizetić, D. Čoko, M. Arici, A.T. Hoang, E. Giama, A. Papadopoulos, Techno-economic and environmental evaluation of photovoltaic-thermal collector design with pork fat as phase change material, *Energy* 254 (2022), 124284.
- [38] M. Hosseinzadeh, M. Sardarabadi, M. Passandideh-Fard, Energy and exergy analysis of nanofluid based photovoltaic thermal system integrated with phase change material, *energy*. 147 (2018) 636–647.
- [39] R.R. Riehl, S. Mancin, Estimation of thermophysical properties for accurate numerical simulation of nanofluid heat transfer applied to a loop heat pipe, *Int. J. Thermofluids* (2022), 100158.
- [40] A.I.A. Al-Musawi, A. Taheri, A. Farzanehnia, M. Sardarabadi, M. Passandideh-Fard, Numerical study of the effects of nanofluids and phase-change materials in photovoltaic thermal (PVT) systems, *J. Therm. Anal. Calorim.* 137 (2019) 623–636.
- [41] G. Asefi, T. Ma, R. Wang, Parametric investigation of photovoltaic-thermal systems integrated with porous phase change material, *Appl. Therm. Eng.* 201 (2022), 117727.
- [42] M. Khodadadi, M. Sheikholeslami, Assessment of photovoltaic thermal unit equipped with phase change material in different finned containers, *J. Energy Storage* 46 (2022), 103939.
- [43] A. Kazemian, A. Salari, A. Hakkaki-Fard, T. Ma, Numerical investigation and parametric analysis of a photovoltaic thermal system integrated with phase change material, *Appl. Energy* 238 (2019) 734–746.
- [44] S. Khanna, S. Paneliya, P. Prajapati, I. Mukhopadhyay, H. Jouhara, Ultra-stable silica/exfoliated graphite encapsulated n-hexacosane phase change nanocomposite: a promising material for thermal energy storage applications, *Energy* 250 (2022), 123729.
- [45] A. Nahar, M. Hasanuzzaman, N.A. Rahim, Numerical and experimental investigation on the performance of a photovoltaic thermal collector with parallel plate flow channel under different operating conditions in Malaysia, *Sol. Energy* 144 (2017) 517–528.
- [46] M. Sardarabadi, M. Passandideh-Fard, Experimental and numerical study of metal-oxides/water nanofluids as coolant in photovoltaic thermal systems (PVT), *Sol. Energy Mater. Sol. Cells* 157 (2016) 533–542.
- [47] S. Alsaqoor, A. Alahmer, F. Al Quran, A. Andruszkiewicz, K. Kubas, P. Regucki, W. Wędrychowicz, Numerical modeling for the retrofit of the hydraulic cooling subsystems in operating power plant, *Therm. Eng.* 64 (2017) 551–558.
- [48] M. Rashad, N. Khordehghah, A. Żabnieńska-Góra, L. Ahmad, H. Jouhara, The utilisation of useful ambient energy in residential dwellings to improve thermal comfort and reduce energy consumption, *Int. J. Thermofluids* 9 (2021), 100059.
- [49] H. Jouhara, A. Żabnieńska-Góra, N. Khordehghah, D. Ahmad, T. Lipinski, Latent thermal energy storage technologies and applications: a review, *Int. J. Thermofluids* 5 (2020), 100039.
- [50] M. Noura, H. Sammouda, Numerical study of an inclined photovoltaic system coupled with phase change material under various operating conditions, *Appl. Therm. Eng.* 141 (2018) 958–975.
- [51] L. Zeng, J. Lu, Y. Li, W. Li, S. Liu, J. Zhu, Numerical study of the influences of geometry orientation on phase change material's melting process, *Adv. Mech. Eng.* 9 (2017), 1687814017720084.
- [52] J. Liu, D. Jiang, H. Fei, Y. Xu, Z. Zeng, W. Ye, Preparation and energy storage properties of a Lauric acid/Octadecanol eutectic mixture, *ACS Omega* 6 (2021) 23542–23550.
- [53] K. Nishioka, T. Hatayama, Y. Uraoka, T. Fuyuki, R. Hagihara, M. Watanabe, Field-test analysis of PV system output characteristics focusing on module temperature, *Sol. Energy Mater. Sol. Cells* 75 (2003) 665–671.
- [54] R. Nasrin, M. Hasanuzzaman, N.A. Rahim, Effect of high irradiation and cooling on power, energy and performance of a PVT system, *Renew. Energy* 116 (2018) 552–569.
- [55] M.M. Rahman, M. Hasanuzzaman, N.A. Rahim, Effects of various parameters on PV-module power and efficiency, *Energy Convers. Manag.* 103 (2015) 348–358.
- [56] W.C. Swinbank, Long-wave radiation from clear skies, *Q. J. R. Meteorol. Soc.* 89 (1963) 339–348.
- [57] W.H. McAdams, *Heat Transmission*, 3rd ed., McGraw-Hill, New York, 1954.
- [58] A. Bejan, *Heat Transfer*, Wiley, New York, 1993.
- [59] Y. Khanjari, A.B. Kasaiean, F. Pourfayaz, Evaluating the environmental parameters affecting the performance of photovoltaic thermal system using nanofluid, *Appl. Therm. Eng.* 115 (2017) 178–187.
- [60] M. Selmi, M.J. Al-Khawaja, A. Marafia, Validation of CFD simulation for flat plate solar energy collector, *Renew. Energy*. 33 (2008) 383–387.
- [61] M.C. Browne, B. Norton, S.J. McCormack, Heat retention of a photovoltaic/thermal collector with PCM, *Sol. Energy*. 133 (2016) 533–548.
- [62] D. Su, Y. Jia, Y. Lin, G. Fang, Maximizing the energy output of a photovoltaic-thermal solar collector incorporating phase change materials, *Energy Build* 153 (2017) 382–391.
- [63] H. Fayaz, N.A. Rahim, M. Hasanuzzaman, A. Rivai, R. Nasrin, Numerical and outdoor real time experimental investigation of performance of PCM based PVT system, *Sol. Energy* 179 (2019) 135–150.
- [64] W. Pang, Q. Zhang, G.J. Wilson, Q. Yang, H. Yan, Empirical influence of various environmental conditions and mass flow rates on hybrid photovoltaic thermal modules, *Appl. Therm. Eng.* 171 (2020), 114965.
- [65] H. Fayaz, N.A. Rahim, M. Hasanuzzaman, R. Nasrin, A. Rivai, Numerical and experimental investigation of the effect of operating conditions on performance of PVT and PVT-PCM, *Renew. Energy*. 143 (2019) 827–841.
- [66] M.S. Hossain, A.K. Pandey, J. Selvaraj, N. Abd Rahim, A. Rivai, V.V. Tyagi, Thermal performance analysis of parallel serpentine flow based photovoltaic/thermal (PV/T) system under composite climate of Malaysia, *Appl. Therm. Eng.* 153 (2019) 861–871.
- [67] A.H.A. Al-Waeli, K. Sopian, M.T. Chaichan, H.A. Kazem, A. Ibrahim, S. Mat, M. H. Ruslan, Evaluation of the nanofluid and nano-PCM based photovoltaic thermal (PVT) system: an experimental study, *Energy Convers. Manag.* 151 (2017) 693–708.